

Dinitrogen Activation and Conversion by Actinide Complexes

Published as part of JACS Au special issue "Advances in Small Molecule Activation Towards Sustainable Chemical Transformation".

Yafei Li,[§] Xiaoqing Xin,[§] Qin Zhu,^{*} and Congqing Zhu^{*}

Cite This: *JACS Au* 2024, 4, 4612–4627

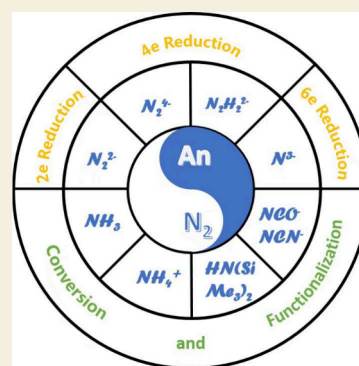
Read Online

ACCESS |

Metrics & More

Article Recommendations

ABSTRACT: The efficient activation and conversion of dinitrogen (N_2) represent a significant challenge in sustainable chemistry, offering potential pathways for synthesizing valuable nitrogen-containing compounds while reducing the environmental impact of traditional nitrogen fixation processes. While transition metal catalysts have been extensively studied for this purpose, actinide complexes have been less explored but have recently emerged as promising candidates due to their unique electronic properties and reactivity. This Perspective systematically examines the recent advances in N_2 activation and conversion mediated by actinide complexes, with a particular focus on their synthesis, mechanistic insights, and catalytic capabilities.



KEYWORDS: N_2 activation, actinide element, uranium, small-molecule activation

1. INTRODUCTION

Nitrogen-containing organic compounds play a crucial role in pharmaceuticals, agriculture, and fine chemicals.^{1–5} Despite the abundance of atmospheric nitrogen (N_2), its direct conversion into nitrogen-containing organic compounds remains a formidable challenge.^{2,4,6} In nature, nitrogen fixation occurs primarily through high-energy processes, such as lightning, and biologically through nitrogenase enzymes in microorganisms.^{7–13} However, these natural processes are insufficient to meet the demands of modern society.

Since Haber's patent for ammonia (NH_3) synthesis in 1909,¹⁴ and the subsequent operation of the first commercial plant in 1913, there have been significant advancements in agriculture and industry. It is estimated that approximately 80% of the ammonia produced by the Haber-Bosch process is used in fertilizers, supporting food production for over half of the global population, which quadrupled during the 20th century.⁴ However, this process requires harsh conditions, particularly high pressure (150–350 atm), which necessitates expensive materials and large-scale plants for economical production. Additionally, the steam reforming part for H_2 production contributes to 1.4% of global CO_2 emissions and roughly 2% of the world's total energy consumption.^{15–17} Therefore, the activation and conversion of N_2 to nitrogen-containing compounds under milder conditions are critical research focuses in modern chemistry.^{18–32}

Historically, uranium and uranium nitride materials were used as heterogeneous catalysts for ammonia production before iron-based catalysts were adopted for the Haber–Bosch process.¹⁴ However, the limited availability of uranium resources and its complex chemistry have constrained further developments in uranium-based N_2 fixation. Dinitrogen, with its strong triple bond (154.2 kcal mol⁻¹), presents a significant challenge for bond cleavage due to its poor σ -donating and π -accepting abilities and its large HOMO–LUMO gap, which resists electron transfer.^{33–35} Therefore, an electron-rich and highly reducing metal center, ideally in a medium-to-low oxidation state, is essential for effective N_2 activation, suggesting the potential of actinide elements.

Encouragingly, an increasing number of low-valent actinide complexes have been reported in recent years,^{36–48} and some of them capable of binding and activating N_2 . The actinide elements, particularly uranium, with its 5f, 6d, and 7s orbitals, can participate in bonding, offering multiple oxidation states.^{49,50} Theoretically, multiple electron reductions of N_2

Received: August 30, 2024
Revised: November 8, 2024
Accepted: November 11, 2024
Published: November 21, 2024



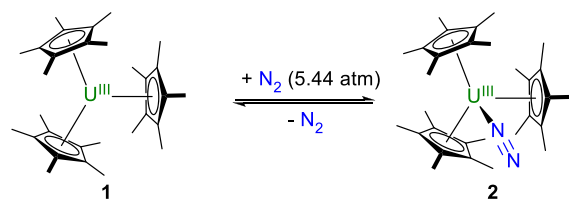
can be achieved through the transformation of low-valent to high-valent actinide complexes via electron transfer.⁵¹

In this review, we systematically summarize the research on N₂ activation and conversion by actinide complexes over the past 30 years. Given the limited reports on thorium–nitrogen complexes, this review primarily focuses on uranium complexes, detailing nitrogen coordination, two-electron, four-electron, and six-electron reduction and conversion.

2. DINITROGEN FIXATION BY ACTINIDE COMPLEXES

Coordinating N₂ to a metal center is a crucial initial step in N₂ activation. In 2003, Evans and co-workers reported an N₂-coordinated complex, [(C₅Me₅)₃U(η¹-N₂)] (**2**), which was synthesized by exposing a solution of the sterically crowded trivalent uranium complex [(C₅Me₅)₃U] (**1**) to N₂ at 5.44 atm (Scheme 1).⁵² The solid-state structure of complex **2** revealed

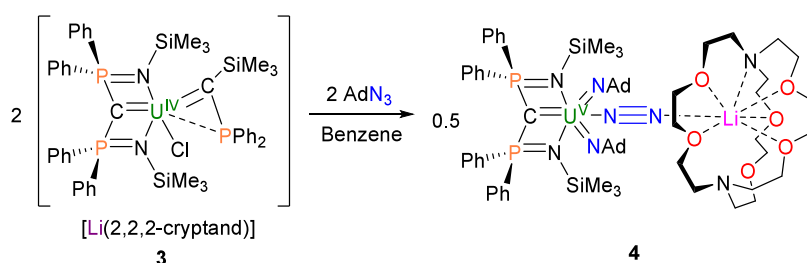
Scheme 1. Synthesis of a Cp*-Supported Mononuclear U(III)–N₂ Complex



that the N₂ ligand adopts a mononuclear end-on (η¹-N₂) binding mode with the uranium center. The N–N bond length in complex **2** (1.120(14) Å) is slightly longer than that in free N₂ (1.0975 Å).⁵³ Additionally, complex **2** readily releases N₂ when the pressure is reduced to 1 atm, indicating a weak interaction between the U center and the N₂ ligand.

N₂ is known to be a weak σ-donor and moderate π-acceptor ligand, making it an unfavorable candidate for coordination with electron-deficient metal centers. However, in 2019, Liddle and colleagues successfully achieved N₂ fixation using a high-valent uranium complex with an electron-poor U(V) metal center.⁵⁴ The U(IV) carbene complex [U{C(SiMe₃)(PPh₂)₂}(BIPM^{TMS})(Cl)][Li(2,2,2-cryptand)] (**3**, BIPM^{TMS} = C-(PPh₂NSiMe₃)₂) was treated with 2 equiv of AdN₃, resulting in the formation of a N₂-bridged dinuclear end-on (μ-η¹:η¹-N₂) complex [U(BIPM^{TMS})(NAd)₂(μ-η¹:η¹-N₂)(Li-2,2,2-cryptand)] (**4**) (Scheme 2). Notably, the N₂ in complex **4** originates from the azide precursor, and the N₂ unit remains electrically neutral. The oxidation state of uranium in complex **4** was confirmed as +V through superconducting quantum interference device (SQUID) magnetometry. The N–N bond length in complex **4** (1.139(9) Å) is slightly elongated

Scheme 2. Synthesis of U(V)–N₂ Complex

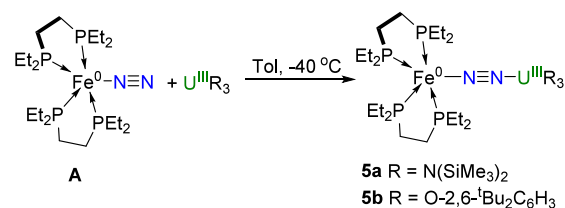


compared to free N₂, and the Raman spectrum exhibits a broad ν(N₂) absorption at approximately 1940 cm⁻¹.

The U ion in complex **4**, being electron-deficient and in a high oxidation state, demonstrates an unusual occurrence of back-bonding with N₂. The authors proposed two possible explanations for this phenomenon.⁵⁴ First, the heterobimetallic uranium–lithium combination may synergistically facilitate N₂ capture, resembling both heterogeneous Haber-Bosch chemistry and homogeneous molecular analogues. Second, the presence of two bonded imido ligands and the tridentate BIPM^{TMS} carbene ligand, acting as π-donors, creates an electron-rich environment around the uranium center, which enhances its ability to engage in π back-bonding with N₂.

Recently, Mazzanti and co-workers used the Fe–N₂ complex [Fe(depe)₂(N₂)] (**A**) (depe = 1,2-bis(diethylphosphino)ethane) to react with trivalent U precursors [U^{III}R₃] (R = N(SiMe₃)₂ or O-2,6-^tBu₂C₆H₃), resulting in the formation of two instances of end-on N₂ bridging U/Fe heterobimetallic complexes **5a** and **5b** (Scheme 3).⁵⁵ The N–N bond lengths in

Scheme 3. Synthesis of N₂-Bridged Fe/U Bimetal Complexes



5a (1.150(7) Å) and **5b** (1.169(7) Å) are slightly longer than that in **A** (1.139(2) Å), and the solid-state IR spectra of **5a** and **5b** exhibit the N≡N triple bond bands at 1833 and 1820 cm⁻¹, respectively. These findings suggest that upon coordination to the U atom, the N₂ ligand is more highly activated compared to **A** (1955 cm⁻¹). Computational studies have revealed a back-bonding covalent contribution to the U(III)–N₂Fe bond, and also indicate that end-on binding of N₂ to U(III) complexes is preferred for the iron-bound N₂ compared to free N₂, likely due to higher polarization.

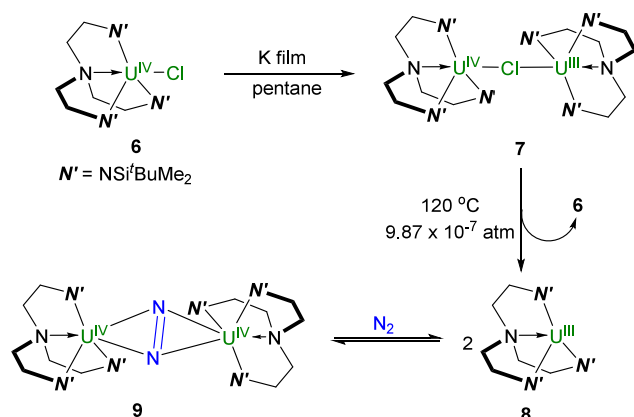
3. TWO-ELECTRON REDUCTION OF N₂ BY ACTINIDE COMPLEXES

The cleavage of the N₂ into reactive intermediates is a challenging process, with the breaking of the first bond being the most critical step. This requires more than 100 kcal mol⁻¹, which accounts for nearly half of the total energy needed to cleave the N≡N triple bond.³³ Since the Scott group first reported a uranium–N₂ complex in 1998,⁵⁶ researchers have increasingly recognized the importance of low-valent uranium

in N₂ activation. The abundant electrons and π -donor capabilities of low-valent U centers, combined with their strong reducing properties, make them particularly effective for this purpose. As a result, the activation of N₂ by low-valent U has become a key focus in actinide chemistry.⁵⁷

In 1998, Scott and co-workers synthesized the species $[\{U(NN')_3\}_2-\mu\text{-Cl}]$ ($NN'_3 = N(\text{CH}_2\text{CH}_2\text{NSi}^t\text{BuMe}_2)_3$) (7) by treating the uranium(IV) chloride precursor $[U(NN'_3)_2\text{Cl}]$ (6) with potassium film.⁵⁶ When the purple pentane solution of 7 was exposed to N₂, it underwent a significant color change to dark red. However, the red material was unstable and could not be isolated for extended study. Inspired by the N₂ activation chemistry observed in zirconium complexes by the Fryzuk group,⁵⁸ the authors carefully sublimated 7 at 120 °C and 9.87×10^{-7} atm to synthesize the trivalent U complex $[U^{III}(NN'_3)]$ (8). When a saturated pentane solution of 8 was exposed to N₂ and cooled to -20 °C, the first example of a uranium N₂ complex $[\{U(NN')_3\}_2(\mu-\eta^2:\eta^2\text{-N}_2)]$ (9) was obtained (Scheme 4).

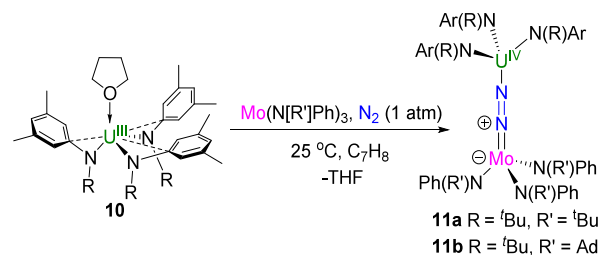
Scheme 4. Synthetic Route to the First Uranium–N₂ Complex



The crystal structure of complex 9 revealed that the N₂ ligand adopts a side-on bridging mode between the two U atoms, with a bond length of 1.109(7) Å between the two N atoms, slightly longer than that in free N₂ (1.0975 Å). This suggests a weak interaction between N₂ and the U centers, consistent with the observation that the N₂ ligand readily decoordinates under vacuum. The UV/visible spectrum and magnetic susceptibility of complexes 8 and 9 were similar, leading the authors to conclude that the coordination of N₂ did not alter the oxidation state of the U centers.⁵⁹ However, subsequent density functional theory (DFT) calculations suggest that complex 9 is best represented as $U(\text{IV})_2\text{N}_2^{2-}$, where the N₂ molecule is reduced by two electrons and the U centers are oxidized.^{60–62}

In 1998, Cummins and co-workers reported a U–Mo heterodinuclear complex featuring a U–N₂ interaction (Scheme 5).⁶³ They synthesized the trivalent uranium complex by reducing the U(IV) precursor $[U(\text{N}[\text{R}]\text{Ar})_3\text{I}]$ ($\text{R} = {}^t\text{Bu}$, $\text{Ar} = 3,5\text{-dimethylphenyl}$) with 1% Na/Hg. The resulting complex (10) showed no reactivity toward N₂ until 1 equiv of $\text{Mo}(\text{N}[\text{R}']\text{Ph})_3$ ($\text{R}' = {}^t\text{Bu}$ or Ad)⁶⁴ was added in toluene under a N₂ atmosphere. This led to the formation of a thermally stable U–Mo heterodinuclear N₂ activation complex $[U(\mu\text{-N}_2)\text{Mo}]$ (11). In this complex, the N₂²⁻ ($d_{\text{NN}} = 1.232(11)$ Å, $\nu_{\text{NN}} = 1568$ cm⁻¹) unit adopts an end-on, linear

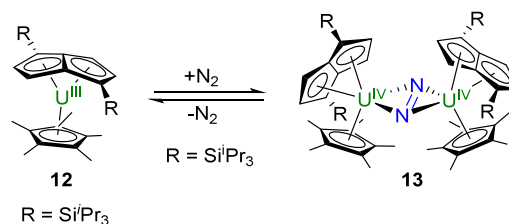
Scheme 5. Synthesis of the U–N₂–Mo Complex



bonding mode, bridging the U^{IV} and Mo^{IV} centers. Based on the crystal structure data, the authors proposed that Mo serves as the more effective π -donor to the complexed N₂ ligand, as depicted in the valence-bond resonance structure in Scheme 5.

Cyclopentadiene ligands are commonly used to stabilize low-valent actinide compounds.^{65–67} The Cloke group utilized $[\text{Cp}^*]^-$ ($\text{Cp}^* = \text{pentamethylcyclopentadiene}$) and a silylated pentalene dianion $[\text{C}_8\text{H}_4\{\text{Si}^i\text{Pr}_3\text{-1,4}\}_2]^{2-}$ as ligands to synthesize a mixed-sandwich U(III) complex $[U^{III}(\eta^5\text{-Cp}^*)(\eta^8\text{-C}_8\text{H}_4\{\text{Si}^i\text{Pr}_3\text{-1,4}\}_2)]$ (12) through a salt elimination reaction in toluene under an argon atmosphere. Exposure of complex 12 to atmospheric pressure N₂ resulted in the formation of a green-black complex $[U^{IV}(\eta^5\text{-Cp}^*)(\eta^8\text{-C}_8\text{H}_4\{\text{Si}^i\text{Pr}_3\text{-1,4}\}_2)(\mu\text{-}\eta^2:\eta^2\text{-N}_2)]$ (13) (Scheme 6).⁶⁸ Despite the reduction of the

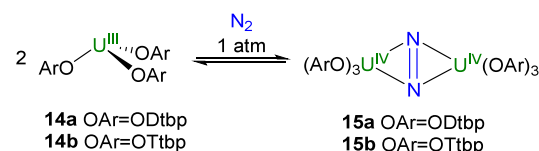
Scheme 6. Synthesis of Complex 13



N₂ molecule in complex 12 to a bridging N₂²⁻ ($d_{\text{NN}} = 1.232(10)$ Å) motif between two U(IV) centers, the complex exhibited high susceptibility to decomposition in both solution and solid states.

The above-discussed N₂ bonding complexes, with the exception of complex 11, generally exhibit instability, often existing in equilibrium between N₂-bound and non-N₂-bound species. In 2011, Arnold group reported a uranium N₂ complex that demonstrates significant stability in both solid-state and solution phases (Scheme 7).⁶⁹ Treatment of $[U^{III}(\text{N}''_3)]$ ($\text{N}'' =$

Scheme 7. Synthesis of Complex 15

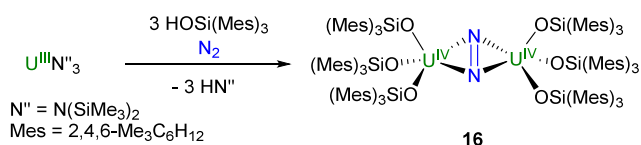


$\text{N}(\text{SiMe}_3)_2$) with 3 equiv of HODtbp or HODipp (OTtbp = 2,4,6-tri-*tert*-butylphenoxide, ODipp = 2,6-diisopropylphenoxide) in hexane under argon respectively yielded two U(III) complexes supported by aryloxy ligands, $[U^{III}(\text{ODtbp})_3]$ (14a) and $[U^{III}(\text{OTtbp})_3]$ (14b). Subsequent exposure to N₂ resulted in the formation of a dimeric species $[U^{IV}(\text{OAr})_3]_2(\mu\text{-}\eta^2:\eta^2\text{-N}_2)$ (15). In this complex, N₂ was reduced to N₂²⁻ and coordinated in a side-on fashion between two U centers. The

bond lengths of N=N in complex **15a** were reported as 1.163(19) Å, 1.204(17) Å, and 1.201(19) Å from three sets of crystal structure data, respectively. The distances of N–N in **15b** were 1.190(18) Å (crystallized from *n*-hexane) and 1.236(5) Å (from toluene). Raman spectroscopy revealed a N₂ stretching vibration at 1451 cm⁻¹ for complex **15b**. DFT calculations by Kaltsoyannis confirmed the formulation of complex **15**, demonstrating strong overall polarity in U–N₂ binding, with a covalent U–N₂ π back-bonding interaction that results in the elongation and weakening of the N₂ bond.

Two years later, the Arnold group reported a similar result. They synthesized a uranium N₂ complex [U^{IV}{OSi(Mes)₃}₃]₂(μ-η²:η²-N₂) (**16**) using bulky trimesitylsiloxide ligands, following a method similar to that used for complex **15** (Scheme 8).⁷⁰ The crystal structure of complex **16** closely

Scheme 8. Synthesis of Complex **16**

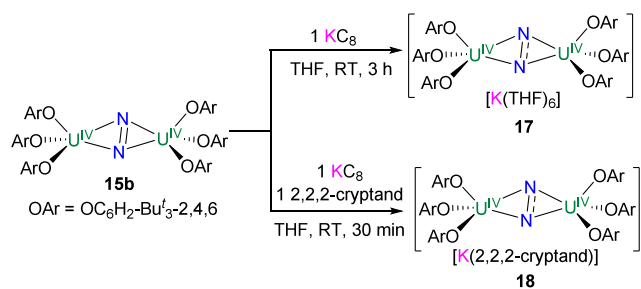


resembles that of **15**, with N₂ reduced to N₂²⁻ and bonding side-on with two [U^{IV}(OSi(Mes)₃)₃] fragments. In comparison to complex **15**, complex **16** exhibited remarkable thermodynamic stability, showing minimal decomposition even when the toluene solution was heated to 100 °C. This underscores the critical role of bulky ligands in enhancing the stability of such compounds.

4. THREE-ELECTRON REDUCTION OF N₂ BY ACTINIDE COMPLEXES

Recently, a three-electron reduction of N₂ was reported by Mazzanti and co-workers.⁷¹ They found that by reducing complex **15b** with 1 equiv of KC₈ or 1 equiv of KC₈ and 1 equiv of 2.2.2-cryptand, the N₂^{•3-}-bridged diuranium complex [K(THF)₆][{(ArO)₃U]₂(μ-η²:η²-N₂)] (**17**) or [K(2.2.2-cryptand)][{(ArO)₃U]₂(μ-η²:η²-N₂)] (**18**) was generated, respectively (Scheme 9). The N–N bond distances in **17**

Scheme 9. Synthesis of N₂^{•3-}-Bridged Diuranium Complexes



and **18** are comparable to that of complex **15b**. The magnetic susceptibility data confirm the three-electron reduction of N₂ to N₂^{•3-}. This represents the only known example of a three-electron reduction of N₂ by an actinide complex, which shows significant potential in the design of molecular magnets.

5. FOUR-ELECTRON REDUCTION OF N₂ BY ACTINIDE COMPLEXES

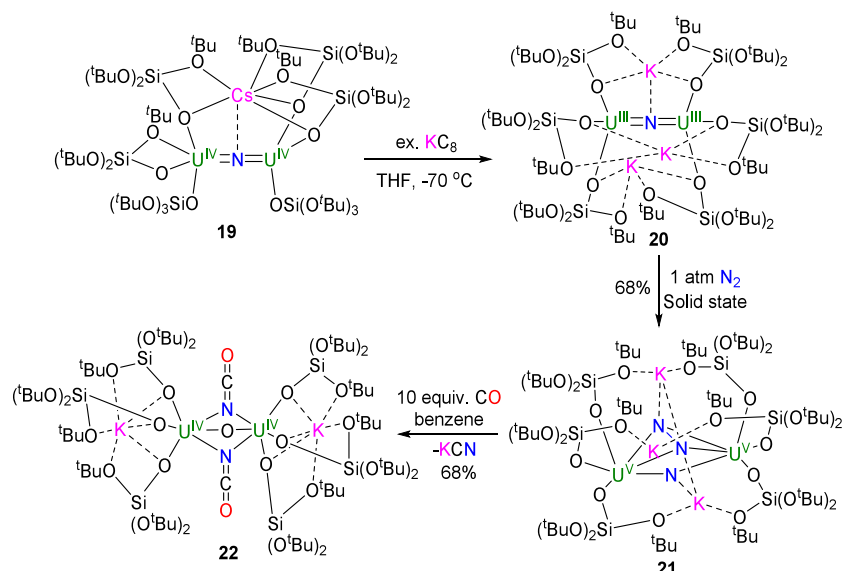
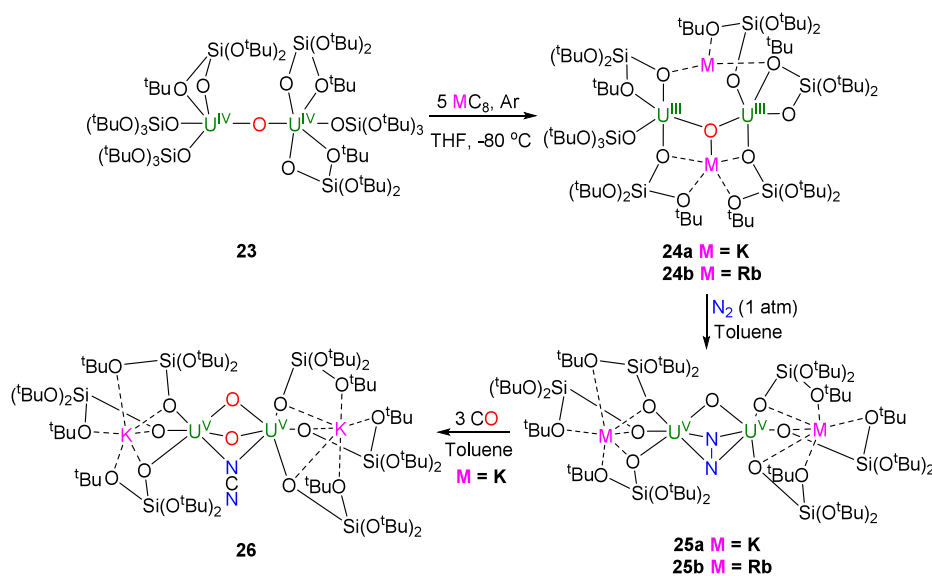
Over the past decade, the Mazzanti group has made significant contributions to the field of N₂ activation, particularly through the use of siloxide-ligand-stabilized multinuclear uranium-alkali metal clusters. In 2017, they reported the first example of a four-electron reduction product of N₂, [K₃{[U^{IV}(OR)₃]₂(μ-N)(μ-η²:η²-N₂)}] (R = Si(O^tBu)₃) (**21**), achieved by exposing the siloxide-stabilized multinuclear U(III)–K cluster [K₃{[U(OR)₃]₂(μ-N)}] (**20**) in a nitrogen atmosphere. Complex **20** was prepared from [Cs{[U(OR)₃]₂(μ-N)}] (**19**)⁷² and KC₈ (Scheme 10).⁷³ In complex **21**, the coordinated N₂ was highly activated and reduced to a N₂⁴⁻ species (*d*_{NN} = 1.521(18) Å). In subsequent studies, they explored functionalization reactions of the N₂⁴⁻ group. The reaction of complex **21** with excess acid (HBAr^F, PyHCl or HCl) produced NH₄Cl with yields ranging from 25% to 42%. Interestingly, when HCl in ether was added to the reaction mixture of complex **21** and H₂, the yield of ammonia increased to 77%. Additionally, treatment of complex **21** with 10 equiv of CO in THF or benzene at room temperature resulted in the isolation of the oxo/cyanate diuranium complex [K₂{[U(OR)₃]₂(μ-O)(μ-NCO)₂}] (**22**) in 68% yield, with the formation of CN⁻ confirmed by ¹³C NMR spectroscopy.

Two years later, they reduced an oxo-bridged complex, [[U^{IV}(OSi(O^tBu)₃)₃]₂(μ-O)] (**23**) with KC₈ at –80 °C, leading to the formation of a U^{III}–K heteronuclear cluster [K₂{[U^{III}(OSi(O^tBu)₃)₃]₂(μ-O)}] (**24a**) (Scheme 11).⁷⁴ Subsequent reaction with N₂ in solution generated the U^{IV}–K heteronuclear N₂-bound complex [K₂{[U^{IV}(OSi(O^tBu)₃)₃]₂(μ-O)(μ-η²:η²-N₂)}] (**25a**). Similar to complex **21**, the N₂⁴⁻ ligand in complex **25a** adopts a side-on bridging mode between two U(V) centers, with a N–N bond length of 1.40(1) Å, which is slightly shorter than that observed in complex **21**. Complex **25a** exhibited exceptional stability in both the solid state and in toluene solution, with no loss of N₂ observed after three cycles of freeze–pump–thaw degassing under argon.

In a subsequent study, they attempted to synthesize heavier analogs (M = Rb, Cs). However, **25b** (M = Rb) showed poor stability, and the Cs analog could not be afforded due to large cation size and low Lewis acidity.⁷⁵ The toluene solution of complex **25a** is exposed to 3 equiv of CO yielding a cyanamido-bridged complex [K₂{[U(OSi(O^tBu)₃)₃]₂(μ-O)₂(μ-NCN)}] (**26**) in 68% yield. Further conversion of **26** with excess CO to N-containing product could not be identified. The addition of excess HCl(Et₂O) to complex **25a** in the presence of 2.1 equiv of 2.2.2-cryptand in THF generated NH₄Cl in 74% yield.⁷⁶

In 2020, Arnold and co-workers carried out the reaction of uranium/thorium complexes (**27**), supported by a phenyl-bridged phenoxide ligand, with potassium graphite under N₂ atmosphere, leading to the formation of N₂ four-electron reduction products (Scheme 12).⁷⁷ In this reaction, complex K₄[U₂(μ-N₂H₂)(mTP⁴⁻)₂] (mTP⁴⁻ = [2-(OC₆H₂-^tBu-2,Me-4)₂CH}-C₆H₄-1,3]⁴⁻) (**28a**) was characterized by X-ray diffraction. During the formation of **28**, hydrogen atoms at the benzyl C-position were abstracted, and the N₂ was reduced, resulting in the formation of an N₂H₂²⁻ motif (*d*_{NN} = 1.491(5) Å in **28a**). However, the Th analogue, **28b**, was not characterized by X-ray diffraction.

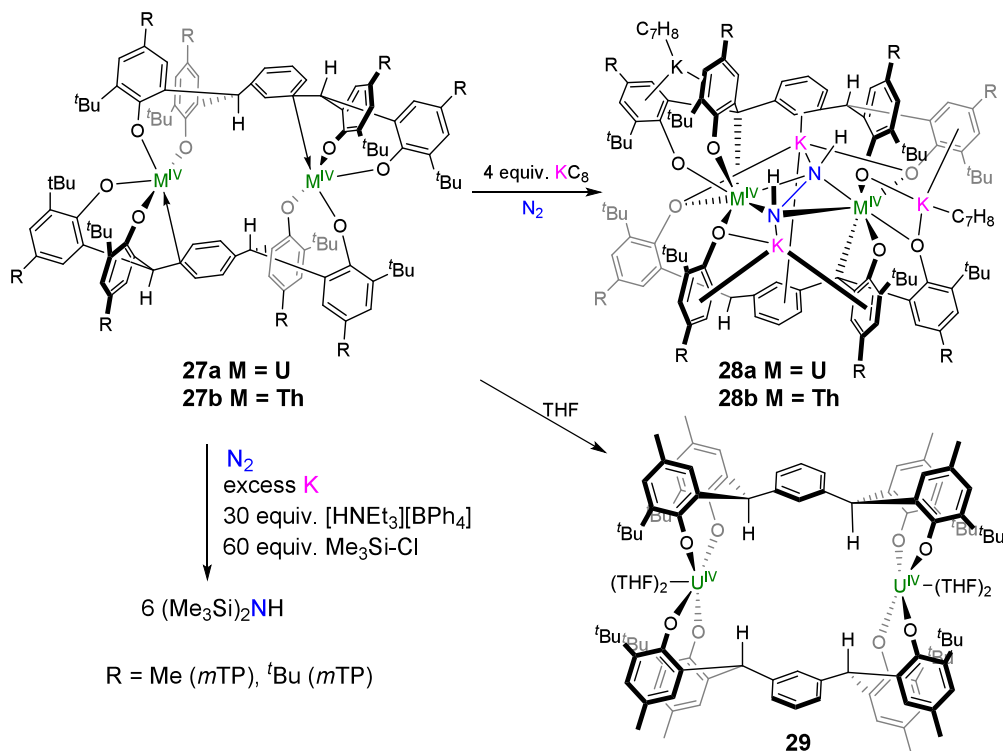
Complex **28a** reacted with strong acid pyridinium chloride or weaker acid [HNEt₃][BPh₄] to produce NH₄Cl. The N₂-

Scheme 10. N₂ Reduction and Functionalization Mediated by 20Scheme 11. N₂ Reduction and Functionalization Mediated by 24

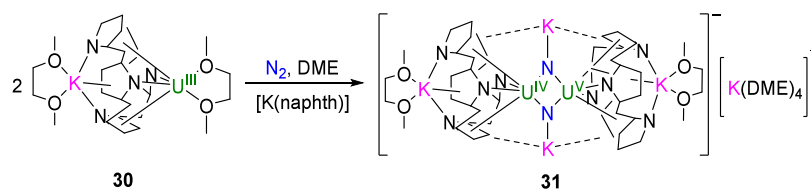
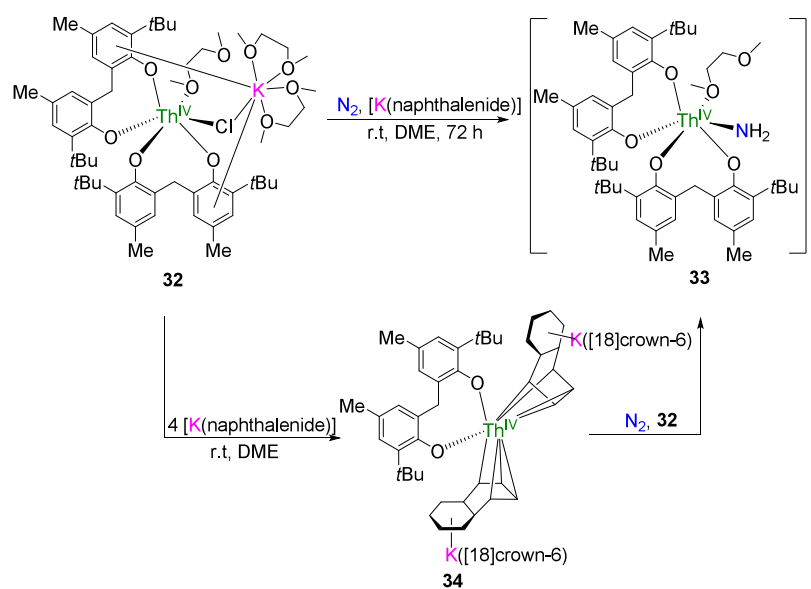
activated complex (**28a**) was capable of catalytically converting molecular N₂ to the secondary silylamine hexamethyldisilazane ((Me₃Si)₂NH) in yields of up to 6.4 equiv per molecule in the presence of excess reductant, weak acid, and chlorosilane at ambient temperature and pressure. NMR spectroscopy and gas chromatography–mass spectrometry (GC-MS) analysis of the nitrogen-containing products confirmed the formation of (Me₃Si)₂NH with high selectivity. Recently, they reported a THF-solvated metallacyclic U(IV) complex with a larger cavity (**29**), prepared from complex **27a** (R = Me) in THF, which can catalyze the conversion of N₂ to (SiMe₃)₂NH and N(Me₃Si)₃ (20.5 ± 1.7 combined equivalents of amine) with excess potassium metal, Me₃SiCl, and weak acid [HNEt₃]-[BPh₄], and to N(Me₃Si)₃ (10.1 ± 1.5 equiv) in the absence of acid.⁷⁸ The release of silylamine did not lead to decomposition of the reaction precursors, which are stabilized by two rigid arene-bridged aryloxy ligands.

6. DINITROGEN CLEAVAGE BY ACTINIDE COMPLEXES

The cleavage of the N≡N bond is significant challenging due to its exceptionally high bond dissociation energy, necessitating a theoretical six-electron reduction for complete cleavage. This demanding process typically requires the involvement of multiple metal centers, in contrast to N₂ cleavage by single U atoms observed in matrix isolation studies.^{79–84} Gambarotta and colleagues reported the first example of N₂ cleavage in the formation of a uranium nitride complex.⁸⁵ They reduced the U–K heterobimetallic complex [(Et₈-calix[4]tetrapyrrole)-U^{III}(dme)][K(dme)] (**30**) with [K(naphthalenide)] in the presence of N₂ in DME, leading to the formation of the anionic μ -nitrido U^V/U^{IV} mixed-valent complex, [(K(dme)(calix[4]-tetrapyrrole)U)₂][K(dme)₄] (**31**) (Scheme 13). In this complex, each nitride bridges two U atoms and a K atom. The U(V) center was confirmed by a characteristic absorption at 1247 nm in the near-IR spectrum. These results suggest that

Scheme 12. Binuclear U and Binuclear Th Complex-Promoted N_2 Activation

Scheme 13. Synthesis of Complex 31

Scheme 14. Synthesis of N_2 Cleavage Product 33

the two U centers contribute three electrons, while the three K ions provide the remaining three electrons necessary for the

six-electron reduction of N_2 , highlighting the essential role of K ions in this process.

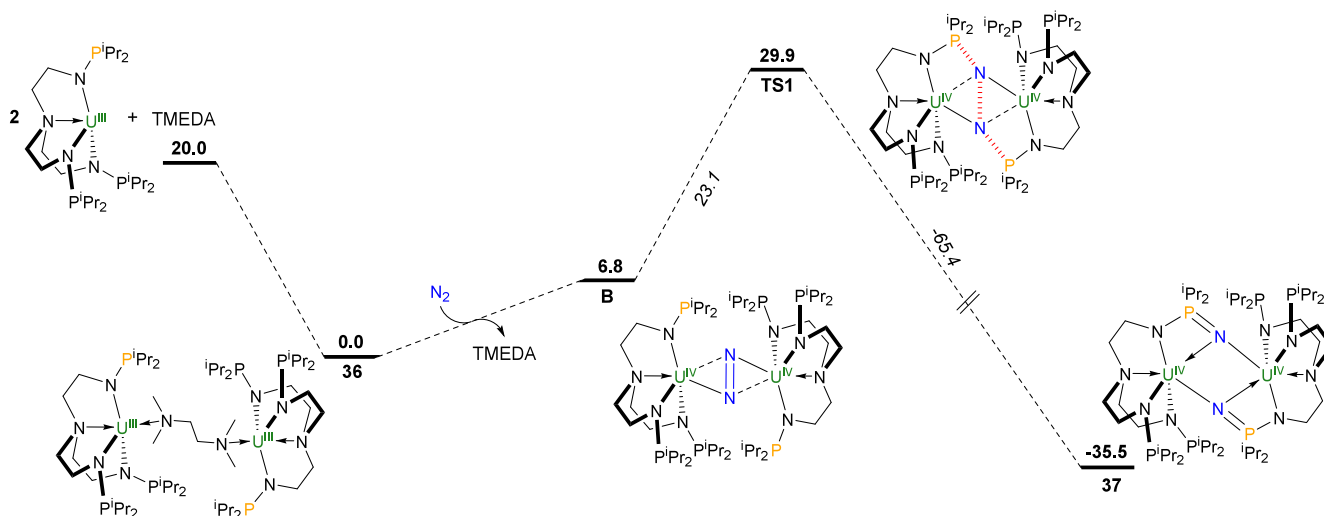
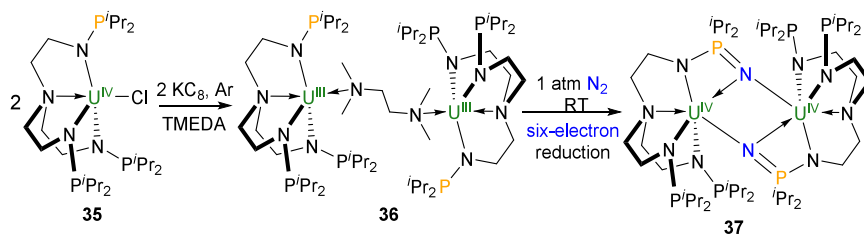
Scheme 15. Cleavage of N₂ through U(III)–P(III) Synergetic Strategy

Figure 1. Computed enthalpy profile (in kcal mol⁻¹) for the formation of complex 37.

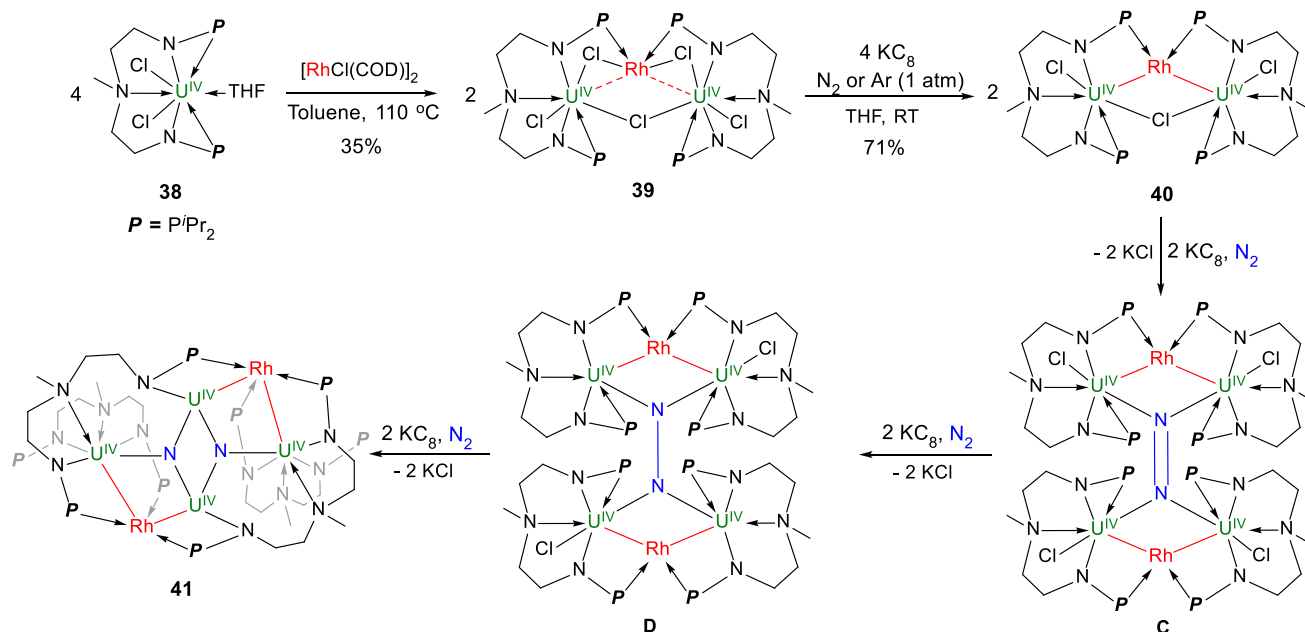
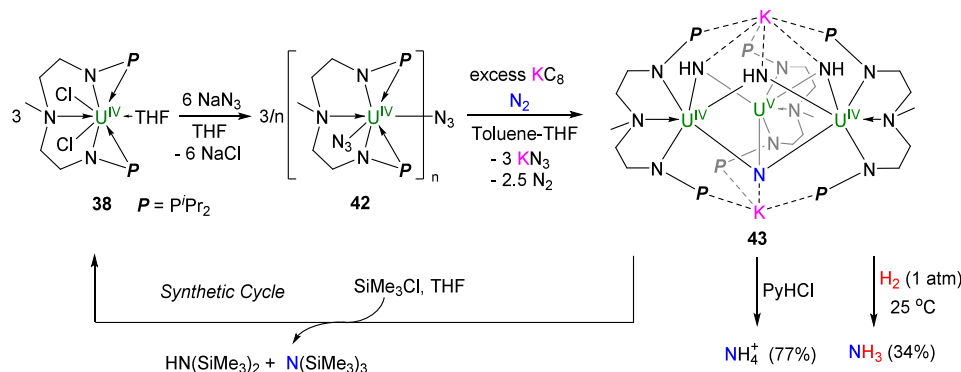
The first instance of N₂ cleavage by a thorium complex was also reported by Gambarotta's group (Scheme 14).⁸⁶ They reduced a Th(IV) complex 32 supported by a diphenol ligand with 1 equiv of [K(naphthalenide)] in DME under N₂, resulting in the formation of a thorium amide complex 33. In this complex, N₂ was transferred to the NH₂⁻ group. The ¹⁵N NMR spectrum of compound 33 confirmed that the N atom in the amino group originated from N₂, evidenced by a sharp triplet peak at 155.01 ppm. The authors proposed that the two hydrogen atoms on the amino group may originate from the solvent through a radical-type hydrogen abstraction process. Additionally, when complex 32 was reacted with 4 equiv of [K(naphthalenide)] in the presence of [18]-crown-6, complex 34 was produced. Complex 34 could be considered a zerovalent synthon or a tetravalent species, though it does not react with N₂ on its own. The authors suggested that interaction between 32 and 34 under N₂ conditions could initiate a process in which N₂ is cleaved and partially hydrogenated to yield complex 33. Arnold and co-workers attempted to reproduce this reaction with a wide variety of conditions, however, no evidence of N₂ binding, reduction, or activation or of ligand deprotonation was observed.⁷⁷

Ligands can assist in the cleavage of N₂ by U centers. In 2020, Zhu group successfully cleaved the N≡N triple bond using a double-layer nitrogen–phosphorus ligand-supported trivalent uranium complex [N-(CH₂CH₂NPⁱPr₂)₃U]₂(TMEDA) (36) (Scheme 15).⁸⁷ This complex was synthesized by reducing the uranium(IV) complex [N(CH₂CH₂NPⁱPr₂)₃UCl] (35) with KC₈. Complex 36 could react with N₂, leading to the formation of product [N(CH₂CH₂NPⁱPr₂)₂(CH₂CH₂NPⁱPr₂N)U]₂ (37) via phosphorus-assisted N₂ cleavage (Scheme 15). In complex 37, a

N=P double bond was formed (*d*_{NP} = 1.617(3) and 1.593(3) Å), indicating that the P atoms in the phosphinimide are in the +V oxidation state, each providing two electrons to the N₂ reduction. Reacting complex 37 with 8 equiv of degassed H₂O yielded a nitrogen-containing organic species [N-(CH₂CH₂NPⁱPr₂)₂(CH₂CH₂NPⁱPr₂NH)] (L-NH) in 55% yield, which could be further hydrolyzed to NH₃ with excess H₂O. The facile two-electron process that oxidizes P(III) to P(V) presents an innovative approach for N₂ reduction and functionalization, although similar processes have been observed in transition metal systems.^{88,89}

A distinct outcome was observed when the silyl group in the triamidoamine ligand was replaced with a trivalent phosphorus group. Unlike in complex 9,⁵⁶ where N₂ was only weakly activated. DFT calculations suggest that the U ions in complex 36 undergo oxidation upon coordination with N₂, resulting in the formation of a U(IV) complex B (Figure 1). At the transition state (TS1), complete reduction of N₂ occurs, followed by a simultaneous trans-attack of the two nitrogen atoms by lone pairs of electrons from the P atoms (one on each uranium unit) positioned above and below the U₂N₂ plane. At TS1, although the N–N bond is not fully broken, both nitrogen atoms are symmetrically bonded to their respective uranium centers.

Previous examples have demonstrated that nitrogen cleavage often requires the collaborative action of multiple metal centers, a condition well-suited to metal clusters. The nitrogen–phosphorus ligands developed by Zhu group were found to be particularly effective in constructing multiple clusters with metal–metal bonds.^{90–96} These multiple metal systems may be used to activate N₂ due to the synergistic coordination effect of the metals. In 2020, they found that the

Scheme 16. N₂ Cleavage Mediated by the Cluster with U–Rh BondsScheme 17. N₂ Cleavage by Uranium Azide Complex 43

N–P ligand-supported uranium–rhodium cluster could be used to cleave N₂ (Scheme 16). By reacting the uranium precursor $\{U[N(CH_3)(CH_2CH_2NP^iPr_2)_2](Cl)_2(THF)\}$ (38) with $[RhCl(COD)]_2$, a trinuclear cluster $[\{U[N(CH_3)(CH_2CH_2NP^iPr_2)_2](Cl)_2(\mu-Cl)(\mu-Rh)\}]$ (39) was obtained (Scheme 16).⁹⁷ Subsequent reduction with excess equivalents of KC₈ resulted in a six-electron N₂ reduction complex $[\{U_2[N(CH_3)(CH_2CH_2NP^iPr_2)_2]_2(Rh)(\mu-N)\}]_2$ (41). By controlling the amounts of KC₈, the intermediate $[\{U[N(CH_3)(CH_2CH_2NP^iPr_2)_2](Cl)_2(\mu-Cl)(\mu-Rh)\}]$ (40) was isolated, which could be further reacted with KC₈ to generate the N₂ cleavage product 41. In complex 41, the N–N distance is 2.780 Å, indicating complete cleavage of the N≡N bond. The N₂-cleaved uranium–rhodium cluster 41 was protonated with an excess of acid, generating substantial yields of ammonium. The ¹⁵N-labeled product confirmed that the two nitride ligands in complex 41 originated from N₂.

Computational analysis indicates that the overall reduction of N₂ from 40 to 41 is exothermic by 40.0 kcal mol^{−1}, with each step of the reduction being thermodynamically favored (Scheme 16). The initial step in the formation of complex 41 from 40 involves a two-electron reduction of N₂ through coordination to the U centers, resulting in the proposed

intermediate C with the release of energy of 23.4 kcal mol^{−1}. The N=N bond is further broken to generate intermediate D (6.3 kcal mol^{−1} from C) through reaction with 2 equiv of KC₈. Further reduction of D with an additional 2 equiv of KC₈ leads to the formation of complex 41, which is exothermic by 10.3 kcal mol^{−1}. This study demonstrates the capability of a multimetallic uranium cluster to effectively facilitate N₂ fixation and reduction, serving as a promising platform for further research in this area.

Zhu and co-workers found that treatment of complex 38 with 3 equiv of NaN₃ resulted in the formation of a one-dimensional chain uranium azide complex 42. Reduction of complex 42 with excess KC₈ in a toluene/THF mixed solvent under an N₂ atmosphere yielded a U–K nitride/imido complex $[\{[U\{N(CH_3)(CH_2CH_2NP^iPr_2)_2\}(\mu-NH)]_3(\mu-N)\}K_2]$ (43) (Scheme 17).⁹⁸ In this complex, the nitrogen atom of the N^{3−} ligand is derived from N₂, and the protons on the imido motifs are derived from the solvent. The hydrogenation of complex 43 with H₂ at atmospheric pressure and room temperature produced NH₃, which could be captured by excess PyHCl to form NH₄Cl.

Treatment of 43 with excess protonic acid also yielded substantial NH₄Cl. The N₂-cleaved product 43 reacted with

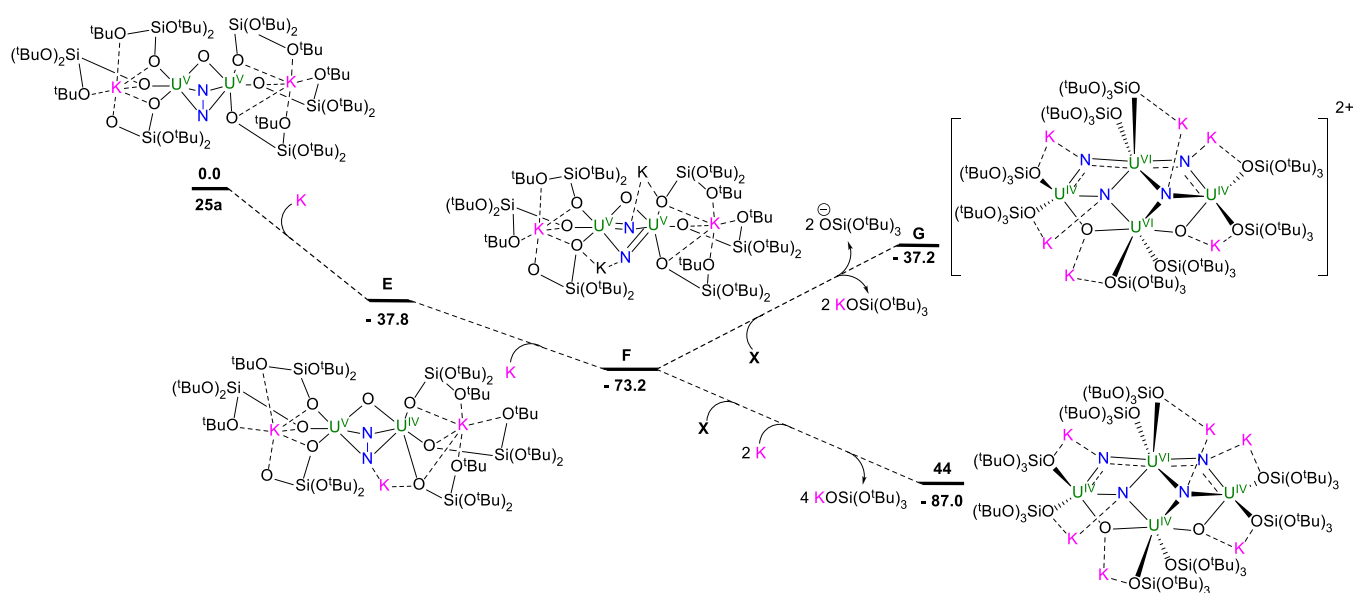
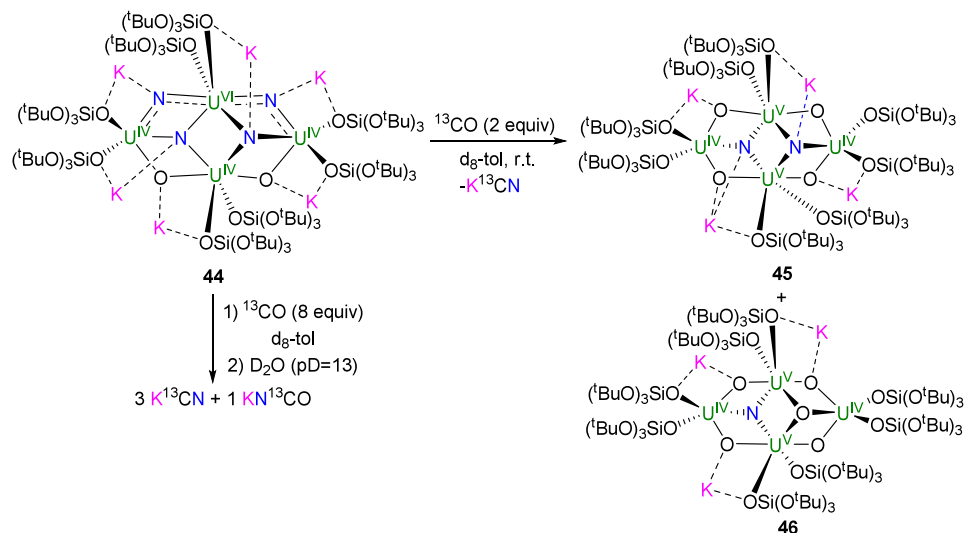
Scheme 18. Functionalization of N₂ Cleavage Product 44

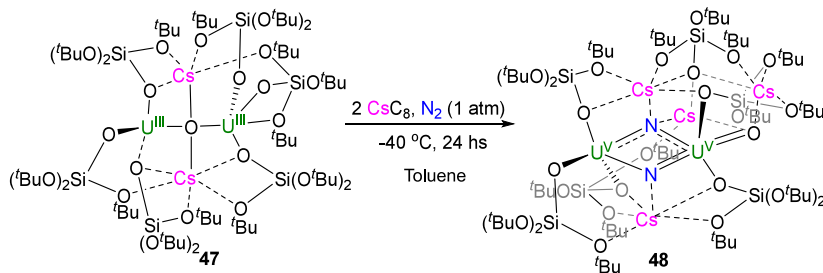
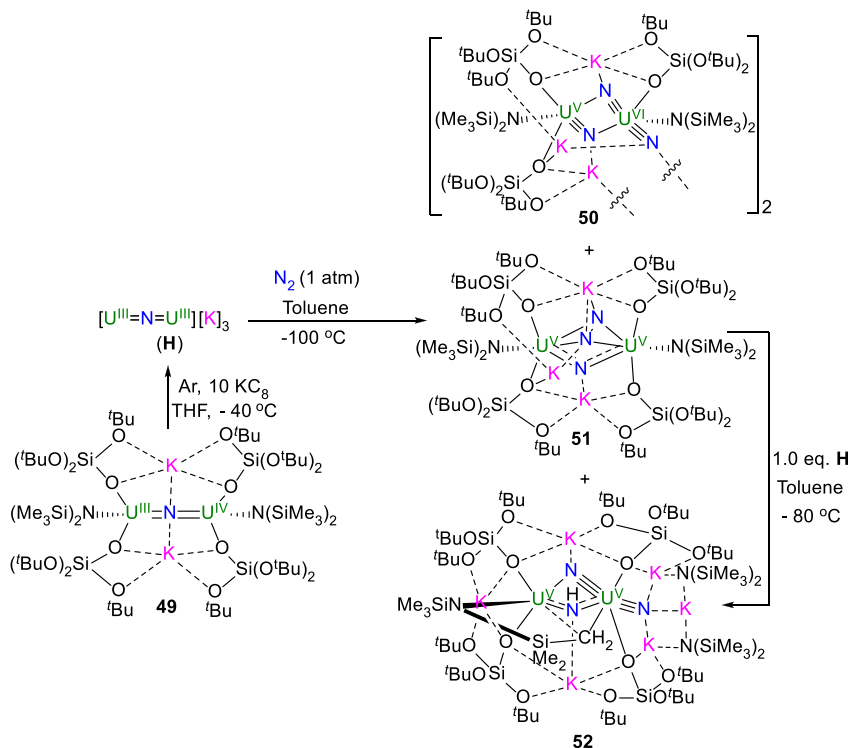
Figure 2. Computed enthalpy profile (in kcal mol⁻¹) for the formation of 44 from 25a.

excess trimethylsilyl chloride (SiMe_3Cl) to generate silylamines ($\text{HN}(\text{SiMe}_3)_2$ and $\text{N}(\text{SiMe}_3)_3$) and the uranium precursor 38, thereby completing a synthetic cycle. The formation of 43 has been elucidated through DFT calculations, which suggest that the synergistic effect between three U centers is important in the $\text{N}\equiv\text{N}$ broken.

By adding 2–4 equiv of KC_8 to a toluene solution of the previously mentioned 25a under N_2 at -40°C , Mazzanti and co-workers successfully synthesized a tetranitride cluster with four uranium centers, $[\text{K}_6\{(\text{OSi}(\text{OtBu})_3)_2\text{U}^{\text{IV}}\}_3\{(\text{OSi}(\text{O}^t\text{Bu})_3)_2\text{U}^{\text{VI}}\}(\mu^4\text{-N})_3(\mu^3\text{-N})(\mu^3\text{-O})_2]$ (44).⁹⁹ In this reaction, the N_2^{4-} unit was cleaved into nitride ligands, resulting in a complex (44) containing three U(IV) and one U(VI) ions, as shown in Scheme 18. Complex 44 reacted with excess HCl to yield NH_4Cl in a quantitative yield of 97%, confirming the presence of four nitride ligands. Additionally, the reactivity of complex 44 with ^{13}CO was investigated. Reaction with 2 equiv of ^{13}CO led to the formation of a mixture of complexes 45 and 46, along with K^{13}CN , as identified by ^{13}C NMR spectroscopy. The structures of 45 and 46 resemble that of complex 44,

where the nitride ligands have been replaced by oxygen ligands with valence redistribution. Further reaction of complex 44 with excess (8 equiv) ^{13}CO yielded K^{13}CN and KN^{13}CO in a 3:1 ratio.

DFT calculations illustrate the formation of compound 44 from 25a (Figure 2). The first step by potassium reduction is predicted to be exothermic by 37.8 kcal mol⁻¹, resulting in a mixed-valence U(V)–U(IV) intermediate E, where K bridges a siloxide ligand and one N atom of the N_2 unit. The N–N bond distance in E is slightly elongated to 1.48 Å, longer than that in 25a (1.40 Å). Subsequent reduction of E with K yields the diuranium(V) bis-nitride F, where natural bond orbital analysis reveals the formation of $\text{U}=\text{N}$ double bonds and $\text{U}-\text{N}$ single bonds at each U center. Further addition of K promotes the dimerization of F, accompanied by the loss of a $\text{KOSi}(\text{O}^t\text{Bu})_3$ per U center, resulting in the exothermic formation of complex 44. These results indicate that only one U(V) ion was oxidized to U(VI), while the remaining three U(V) ions were reduced to U(IV). KC_8 acts as the electron donor in this process. According to ^1H NMR and computational studies, the authors

Scheme 19. Synthesis of N₂ Cleavage Product 48Scheme 20. N₂ Cleavage by the Reduction of 49

proposed that the reaction proceeds via successive one-electron transfers from potassium first to the U center and then to the bound N₂⁴⁻ ligand in complex 25a. This electron transfer induces N–N bond cleavage, suggesting that potassium binding to the N₂⁴⁻ ligand facilitates this cleavage.

As shown in Scheme 11, complex 23 can react with MC₈ (M = K, Rb) under N₂ atmosphere to produce a four-electron reduction product. Mazzanti and co-workers reported the formation of an oxide-bridged dinuclear multimetallic U(III) complex, [Cs₂{U^{III}(OSi(O^tBu)₃)₂(μ-O)}] (47), via the reaction of 23 with 5 equiv of CsC₈ under argon at -80 °C. This complex was then treated with an additional 2 equiv of CsC₈ under a N₂ atmosphere at -40 °C for 1 day, yielding a N₂ cleavage complex, [Cs₃{U^V(OSi(O^tBu)₃)₂(μ-N)}₂{U^V(OSi(O^tBu)₃)₂(κ-O)}][CsOSi(O^tBu)₃] (48) (Scheme 19). In complex 48, two U atoms underwent oxidation to a + V state from + III and were bridged by two μ₃-/μ₄-nitride ligands. Consequently, two additional electrons were provided by Cs during the N₂ cleavage process. This highlights the crucial role of alkaline earth metal cations in the activation of N₂. By the addition of excess HCl(Et₂O) to the complex 48, 100% yield of NH₄Cl was formed. The reaction of 48 with excess ¹³C¹⁸O quenched in D₂O led to the formation of Cs¹³CN and

CsN¹³CO in a 1:1 ratio as determined by the ¹³C NMR spectrum.

Using mixed ligands of OSi(O^tBu)₃⁻ and N(SiMe₃)₂⁻, Mazzanti and co-workers synthesized a nitride-bridged mixed-valence U–K cluster [K₂{U^{IV/III}(OSi(O^tBu)₃)₂(N(SiMe₃)₂)₂(μ-N)}] (49). Subsequent reduction of 49 with 10 equiv of KC₈ under argon at -40 °C yielded a putative U(III) nitride species (H). However, the crystal structure of H remains unknown. When exposed to an N₂ atmosphere at -100 °C, the authors successfully isolated a U(VI)/U(V) trinitride complex, [K₃{U^{VI}(OSi(O^tBu)₃)₂(N(SiMe₃)₂)₂(≡N)}(μ-N)₂{U^V(OSi(O^tBu)₃)₂(N(SiMe₃)₂)}]} (50), as well as (51), and a U(V)/U(V) bis-nitride imido cyclometalated product, [K₄{(OSi(O^tBu)₃)₂U^V(≡N)}(μ-NH)(μ-κ²:C,N-CH₂SiMe₂NSiMe₃){U^V(OSi(O^tBu)₃)₂}[K(N(SiMe₃)₂)₂] (52), respectively (Scheme 20).¹⁰⁰ It is noteworthy that complexes 51 and 52 cannot always be isolated using this method. However, the addition of 1 equiv of *in situ* generated H to the toluene-d₈ solution of 51 afforded 52 in 51% NMR yield. In complexes 50 and 52, N₂ was cleaved to nitride, forming U≡N bonds. Adding HCl(Et₂O) to complex 51 or the reaction mixture of complex 51 and H did not result in the formation of NH₄Cl.

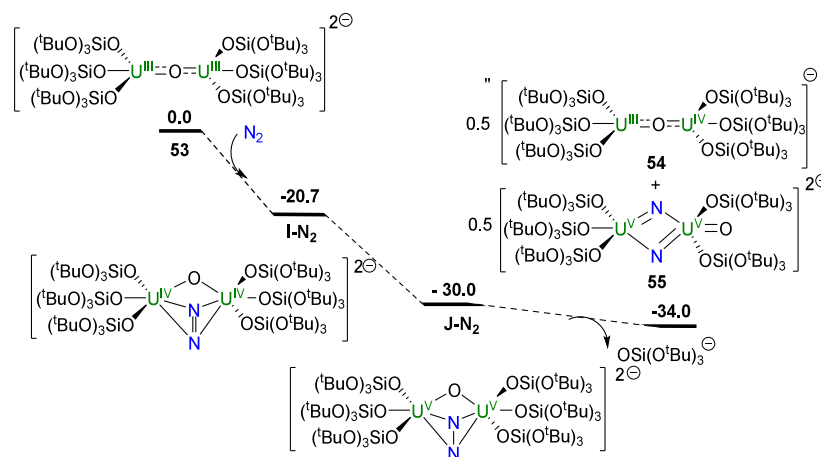
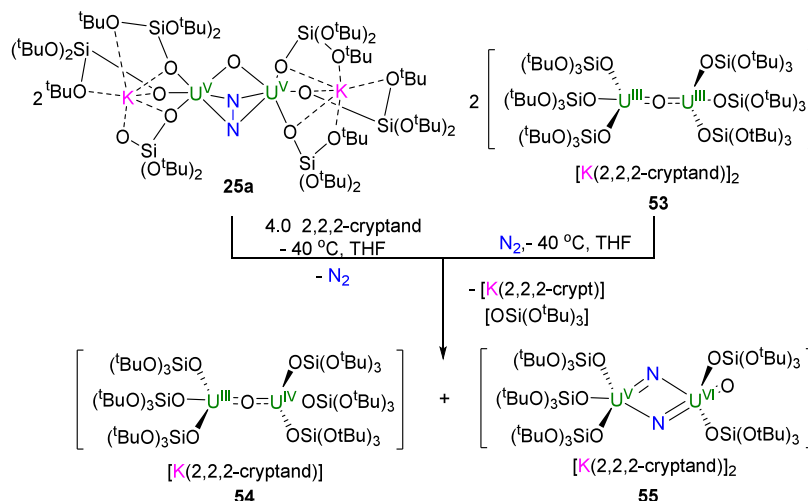
Scheme 21. N₂ Cleavage and Functionalization by 25a and 53

Figure 3. Computed enthalpy (in kcal mol⁻¹) profiles for the formation of 54 and 55.

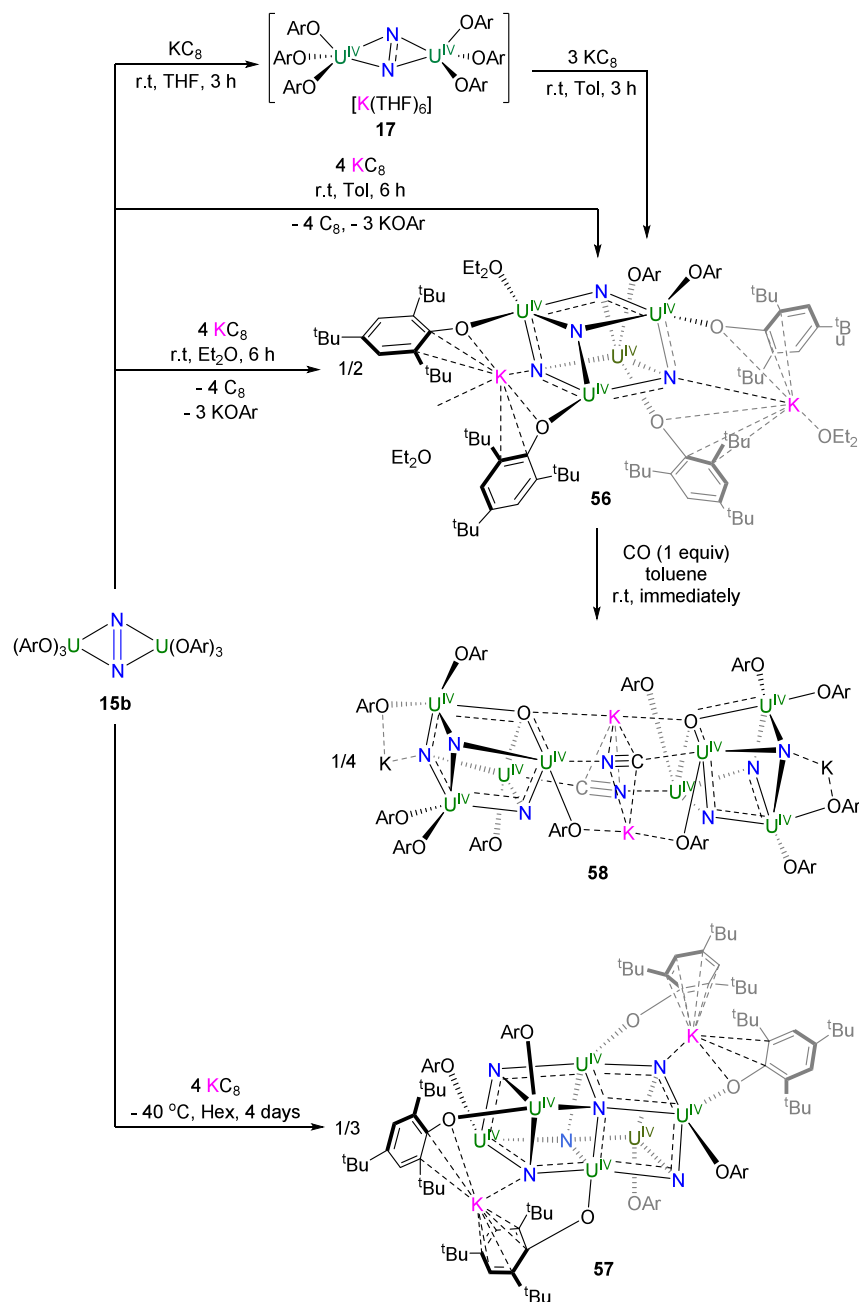
To explore N₂ activation solely by U centers, Mazzanti et al. exposed the alkali metal ion-sequestered oxide-bridged dinuclear U^{III} complex [K(2.2.2-cryptand)]₂[(^tBuO)₃SiO(OSi(O^tBu)₃)₃(μ-O)] (53) to N₂ at -40 °C. This reaction yielded an oxide-bridged U^{III}/U^{IV} dinuclear complex, [K(2.2.2-cryptand)]₂[(^tBuO)₃SiO(OSi(O^tBu)₃)₃(μ-O){U^{IV}(OSi(O^tBu)₃)₃}] (54) and a bis-nitride, terminal-oxo complex [K(2.2.2-cryptand)]₂[(^tBuO)₃SiO(OSi(O^tBu)₃)₃(μ-N)₂{U^{VI}(OSi(O^tBu)₃)₂(κ-O)}] (55) (Scheme 21).⁷⁶ The U–N distances in complex 55 are 1.950(7) and 1.892(8) Å for the U=N double bond, and 2.315(8) and 2.251(7) Å for the U–N single bond, respectively. The molecular structure of complex 55 is similar to that of 48, and the reduction potential measured for complex 53 is greater than that of 24a but similar to 47, although an additional 2 equiv of reducing agent was required. This suggests that alkali ions hinder N₂ binding and further activation. Removing K⁺ from complex 25a through the addition of 2 equiv of 2,2,2-cryptand under N₂ atmosphere at -40 °C produced complexes 54 and 55, similar to the reaction of 53 with N₂. These results suggest that complete sequestration of K⁺ cations could enhance the reducing ability of uranium complexes. The addition of excess HCl to the reaction mixture of complex 53 and N₂ resulted in substantial NH₄Cl formation, as confirmed by ¹⁵N₂-labeling experiments. The addition of ¹³CO to the reaction mixture, followed by

quenching with D₂O yielded N¹³CO⁻ and ¹³CN⁻ as evidenced by ¹³C NMR spectroscopy. The reaction of complex 55 with excess HCl/Et₂O yielded NH₄Cl in 92% yield.

DFT calculations were conducted to elucidate the N₂ reduction pathways facilitated by complex 53 (Figure 3). The results reveal that N₂ undergoes three consecutive two-electron reductions, leading to the formation of intermediates I–N₂ and J–N₂, ultimately yielding complexes 54 and 55. Importantly, each step of this reduction process is thermodynamically favorable.

Recently, Mazzanti group further investigated the reactivity of a uranium–nitrogen complex 15b, previously reported by Arnold group.⁶⁹ Treatment of 15b with 4 equiv of KC₈ in diethyl ether or toluene solution at -40 °C under N₂ yielded a tetranitride cluster [(Et₂O)K]₂(Et₂O)U^{IV}₄(μ-N)₄(OAr)₆ (56) and it can also be synthesized by reacting 17 with 3 equiv of KC₈ in a toluene solution.⁷¹ When the reaction was conducted in *n*-hexane, a hexanitride cluster [K₂{U^{IV}₆(μ-N)₆(OAr)₈}] (57) was formed (Scheme 22). In both complexes 56 and 57, the N–N double bonds were cleaved, resulting in nitride ligands. The U₄N₄ cubane cluster 56 and the U₆N₆ edge-shared cubane cluster 57 reacted with excess HCl/Et₂O to yield quantitative amounts of ammonia. Additionally, the addition of ¹³CO to 56 in toluene-d₈ resulted in quantitative conversion of nitrides to cyanides. The authors

Scheme 22. Synthesis of the Tetranitride (56) and Hexanitride (57) Clusters



also isolated a CN-bridged cluster aggregate with the formula $[\{\text{K}\{\text{U}^{\text{IV}}_4(\mu\text{-N})_3(\mu\text{-O})\}(\text{OAr})_6\}_2(\mu\text{-K})_2(\mu\text{-}\eta^1:\eta^1\text{-CN})_2]$ (**58**), which was produced by the reaction of complex **56** with 1 equiv of ^{13}CO . A protonation experiment of **58** with HCl and D_2O resulted in the formation of NH_4Cl (94%) and $^{13}\text{CN}^-$ (2 equiv), respectively.

7. CONCLUSION AND FUTURE PERSPECTIVE

Nitrogen-containing compounds are pivotal in fields such as agriculture, biology, pharmacology, and materials science. However, the conversion of N_2 into more valuable N-containing products remains a significant challenge in both chemistry and industry. Although actinide complexes have demonstrated substantial potential in N_2 activation, only a limited number of these complexes have successfully converted N_2 into N-containing compounds. These complexes are

capable of activating N_2 into N_2^{2-} , N_2^{3-} , N_2^{4-} , N^{3-} , and $(\text{N}_2\text{H}_2)^{2-}$ species, which can then be further transformed by specific electrophiles such as protons, CO, and silyl reagents to produce NH_3 , CN^- , cyanate, and silylamines. However, direct functionalization of N_2 into N-containing organic compounds has yet to be accomplished. Therefore, a significant challenge is to deepen our understanding of N_2 fixation mechanisms and the N-atom transfer process, which could help in controlling the formation of N-containing products.

Ligands play a crucial role in modifying the steric and electronic properties of metal complexes, which is essential for understanding their structure–reactivity relationships. The ligands employed in the construction of actinide complexes for N_2 activation can be categorized into cyclopentadienyl-type ligands, triamidoamines, amide-type ligands, aryloxides, tetrapyrrole, siloxides, nitrogen–phosphorus ligands, and silyl

phosphino-carbene ligands. These ligands stabilize low- or high-valent actinide complexes, facilitating N₂ activation and adopting varied coordination modes. Rational design of these ligands is crucial to stabilize the low-valent actinide complexes for N₂ activation.

Uranium complexes, in particular low-valent uranium species, have shown exceptional performance in N₂ binding, activation, and cleavage. However, their catalytic potential is limited by the inherent instability of these complexes. To address this, there is a need to explore new systems with strong reducing capabilities that can activate bound N₂ and facilitate N-atom transfer without requiring additional reducing agents under mild conditions. Particularly, multimetallic systems offer diverse coordination modes and synergistic effects for N₂ activation. Moreover, other actinide metals in the tetravalent oxidation state struggle to reduce or form stable reduced intermediates capable of reacting with inert N₂. In this regard, metal–ligand cooperativity should be a central consideration in ligand design. Despite significant advancements in uranium's N₂ chemistry over the past three decades, future research in this area should focus on several key aspects:

Only uranium complexes have been extensively explored in the context of N₂ activation and conversion. Extending N₂ chemistry to thorium and other transuranium elements is crucial for the broader field of actinide chemistry.

Biological nitrogenase metalloenzymes achieve this challenging conversion at ambient temperature and pressure, suggesting that multimetallic cooperativity warrants further investigation in N₂ activation and functionalization.

While numerous activated N₂ metal complexes have been reported, the functionalization of N₂ into N-containing products remains limited. The transfer of nitrogen atoms from these complexes may benefit from photochemical and electrochemical approaches.

Mechanistic studies of N₂ activation and transformation processes are vital for enhancing the selectivity and diversity of N-containing products. Direct catalytic conversion of N₂ into N-containing organic compounds (beyond NH₃ and amines) under mild conditions may become achievable in the future.

The research discussed demonstrates the capability of uranium complexes to facilitate the cleavage and functionalization of N₂ under relatively mild conditions. These breakthroughs point toward a future where actinide metals could play a crucial role in N₂ fixation processes. While significant challenges remain, the potential of actinide metals in the activation and conversion of N₂ is undeniably promising. Continued research in this area is essential and will likely lead to significant advancements, ultimately making the mild conditions for N₂ activation and conversion a realizable goal.

AUTHOR INFORMATION

Corresponding Authors

Qin Zhu – State Key Laboratory of Coordination Chemistry, Jiangsu Key Laboratory of Advanced Organic Materials, School of Chemistry and Chemical Engineering, Nanjing University, Nanjing 210023, China; Email: zhuqin@nju.edu.cn

Congqing Zhu – State Key Laboratory of Coordination Chemistry, Jiangsu Key Laboratory of Advanced Organic Materials, School of Chemistry and Chemical Engineering, Nanjing University, Nanjing 210023, China; orcid.org/0000-0003-4722-0484; Email: zcq@nju.edu.cn

Authors

Yafei Li – State Key Laboratory of Coordination Chemistry, Jiangsu Key Laboratory of Advanced Organic Materials, School of Chemistry and Chemical Engineering, Nanjing University, Nanjing 210023, China

Xiaoqing Xin – School of Medicine, Nanjing University of Chinese Medicine, Nanjing 210023, China

Complete contact information is available at:

<https://pubs.acs.org/10.1021/jacsau.4c00793>

Author Contributions

[§]Y.L. and X.X. contributed equally. CRediT: **Yafei Li** data curation, formal analysis, writing - original draft; **Xiaoqing Xin** data curation, formal analysis, writing - original draft; **Qin Zhu** conceptualization, formal analysis, writing - original draft, writing - review & editing; **Congqing Zhu** conceptualization, funding acquisition, project administration, supervision, writing - review & editing.

Funding

This research was supported by the National Key R&D Program of China (2021YFA1502500), the National Natural Science Foundation of China (22271138, 22401142, and 22301141), the Natural Science Foundation of Jiangsu Province (BK20220065), and the Fundamental Research Funds for the Central Universities (020514380329).

Notes

The authors declare no competing financial interest.

REFERENCES

- (1) Chen, J. G.; Crooks, R. M.; Seefeldt, L. C.; Bren, K. L.; Bullock, R. M.; Darensbourg, M. Y.; Holland, P. L.; Hoffman, B.; Janik, M. J.; Jones, A. K.; Kanatzidis, M. G.; King, P.; Lancaster, K. M.; Lyman, S. V.; Pfromm, P.; Schneider, W. F.; Schrock, R. R. Beyond fossil fuel-driven nitrogen transformations. *Science* **2018**, *360*, No. eaar6611.
- (2) Lv, Z.-J.; Wei, J.; Zhang, W.-X.; Chen, P.; Deng, D.; Shi, Z.-J.; Xi, Z. Direct transformation of dinitrogen: synthesis of N-containing organic compounds via N-C bond formation. *Natl. Sci. Rev.* **2020**, *7*, 1564–1583.
- (3) Masero, F.; Perrin, M. A.; Dey, S.; Mougel, V. Dinitrogen fixation: rationalizing strategies utilizing molecular complexes. *Chem.—Eur. J.* **2021**, *27*, 3892–3928.
- (4) Forrest, S. J. K.; Schluschaß, B.; Yuzik-Klimova, E. Y.; Schneider, S. Nitrogen fixation via splitting into nitrido complexes. *Chem. Rev.* **2021**, *121*, 6522–6587.
- (5) Fang, H.; Ling, Z.; Fu, X. N-H bond activation of ammonia by transition metal and main group element complexes. *Chin. J. Org. Chem.* **2013**, *33*, 738–748.
- (6) Kim, S.; Loose, F.; Chirik, P. J. Beyond Ammonia: nitrogen–element bond forming reactions with coordinated dinitrogen. *Chem. Rev.* **2020**, *120*, 5637–5681.
- (7) Kirn, J. S.; Rees, D. C. Crystallographic structure and functional implications of the nitrogenase molybdenum iron protein from *Azotobacter vinelandii*. *Nature* **1992**, *360*, 553–560.
- (8) Kim, J. S.; Rees, D. C. Structural models for the metal centers in the nitrogenase molybdenum-iron protein. *Science* **1992**, *257*, 1677–1682.
- (9) Georgiadis, M. M.; Komiya, H.; Chakrabarti, P.; Woo, D.; Kornuc, J. J.; Rees, D. C. Crystallographic structure of the nitrogenase iron protein from *azotobacter vinelandii*. *Science* **1992**, *257*, 1653–1659.
- (10) Einsle, O.; Tezcan, F. A.; Andrade, S. L. A.; Schmid, B.; Yoshida, M.; Howard, J. B.; Rees, D. C. Nitrogenase MoFe-protein at 1.16 Å resolution: a central ligand in the FeMo-cofactor. *Science* **2002**, *297*, 1696–1700.

- (11) Einsle, O.; Rees, D. C. Structural enzymology of nitrogenase enzymes. *Chem. Rev.* **2020**, *120*, 4969–5004.
- (12) Foster, S. L.; Bakovic, S. I. P.; Duda, R. D.; Maheshwari, S.; Milton, R. D.; Minteer, S. D.; Janik, M. J.; Renner, J. N.; Greenlee, L. F. Catalysts for nitrogen reduction to ammonia. *Nat. Catal.* **2018**, *1*, 490–500.
- (13) Guo, J.; Wang, M.; Xu, L.; Li, X.; Iqbal, A.; Sterbinsky, G. E.; Yang, H.; Xie, M.; Zai, J.; Feng, Z.; Cheng, T.; Qian, X. Bioinspired activation of N₂ on asymmetrical coordinated Fe grafted 1T MoS₂ at room temperature. *Chin. J. Chem.* **2021**, *39*, 1898–1904.
- (14) Haber, F. Verfahren zur Herstellung von Ammoniak durch katalytische Vereinigung von Stickstoff und Wasserstoff, zweckmäßig unter hohem Druck. DE 229126, 1909.
- (15) Schrock, R. R. Molybdenum does it again. *Nat. Chem.* **2011**, *3*, 95–96.
- (16) Wang, M.; Khan, M. A.; Mohsin, I.; Wicks, J.; Ip, A. H.; Sumon, K. Z.; Dinh, C.-T.; Sargent, E. H.; Gates, I. A.; Kibria, M. G. Can sustainable ammonia synthesis pathways compete with fossil-fuel based Haber-Bosch processes? *Energy Environ. Sci.* **2021**, *14*, 2535–548.
- (17) Smith, C.; Hill, A. K.; Torrente-Murciano, L. Current and future role of Haber–Bosch ammonia in a carbon-free energy landscape. *Energy Environ. Sci.* **2020**, *13*, 331–344.
- (18) Wang, Q.; Guo, J.; Chen, P. The impact of alkali and alkaline earth metals on green ammonia synthesis. *Chem* **2021**, *7*, 3203–3220.
- (19) Liu, T.-T.; Zhai, D.-D.; Guan, B.-T.; Shi, Z.-J. Nitrogen fixation and transformation with main group elements. *Chem. Soc. Rev.* **2022**, *51*, 3846–3861.
- (20) Chen, X.; Xu, H.; Shi, X.; Wei, J.; Xi, Z. Dinitrogen activation and transformation promoted by rare earth and actinide complexes. *Acta Chim. Sin.* **2022**, *80*, 1299–1308.
- (21) Wu, L.-J.; Wang, Q.; Guo, J.; Wei, J.; Chen, P.; Xi, Z. From dinitrogen to N-containing organic compounds: using Li₂CN₂ as a synthon. *Angew. Chem., Int. Ed.* **2023**, *62*, No. e202219298.
- (22) Wang, G.-X.; Wang, X.; Jiang, Y.; Chen, W.; Shan, C.; Zhang, P.; Wei, J.; Ye, S.; Xi, Z. Snapshots of early-stage quantitative N₂ electrophilic functionalization. *J. Am. Chem. Soc.* **2023**, *145*, 9746–9754.
- (23) Yin, Z.-B.; Wu, B.; Wang, G.-X.; Wei, J.; Xi, Z. Dinitrogen functionalization affording chromium diazenido and side-on η²-hydrazido complexes. *J. Am. Chem. Soc.* **2023**, *145*, 7065–7070.
- (24) Klopsch, I.; Kinauer, M.; Finger, M.; Würtele, C.; Schneider, S. Conversion of dinitrogen into acetonitrile under ambient conditions. *Angew. Chem., Int. Ed.* **2016**, *55*, 4786–4789.
- (25) Shima, T.; Zhuo, Q.; Hou, Z. Dinitrogen activation and transformation by multimetallic polyhydride complexes. *Coord. Chem. Rev.* **2022**, *472*, No. 214766.
- (26) Zhuo, Q.; Yang, J.; Zhou, X.; Shima, T.; Luo, Y.; Hou, Z. Aza-Michael addition of dinitrogen to α, β-unsaturated carbonyl compounds in a dititanium framework. *J. Am. Chem. Soc.* **2023**, *145*, 22803–22813.
- (27) Shima, T.; Zhuo, Q.; Zhou, X.; Wu, P.; Owada, R.; Luo, G.; Hou, Z. Hydroamination of alkenes with dinitrogen and titanium polyhydrides. *Nature* **2024**, *632*, 307–312.
- (28) McWilliams, S. F.; Broere, D. L. J.; Halliday, C. J. V.; Bhutto, S. M.; Mercado, B. Q.; Holland, P. L. Coupling dinitrogen and hydrocarbons through aryl migration. *Nature* **2020**, *584*, 221–226.
- (29) Zhuo, Q.; Yang, J.; Zhou, X.; Shima, T.; Luo, Y.; Hou, Z. Dinitrogen cleavage and multicoupling with isocyanides in a dititanium dihydride framework. *J. Am. Chem. Soc.* **2024**, *146*, 10984–10992.
- (30) Zhuo, Q.; Zhou, X.; Shima, T.; Hou, Z. Dinitrogen activation and addition to unsaturated C–E (E = C, N, O, S) bonds mediated by transition metal complexes. *Angew. Chem., Int. Ed.* **2023**, *62*, No. e202218606.
- (31) Wang, Q.; Guo, J.; Chen, P. The impact of alkali and alkaline earth metals on green ammonia synthesis. *Chem.* **2021**, *7*, 3203–3220.
- (32) Liu, T.-T.; Zhai, D.-D.; Guan, B.-T.; Shi, Z.-J. Nitrogen fixation and transformation with main group elements. *Chem. Soc. Rev.* **2022**, *51*, 3846–3861.
- (33) Bazhenova, T. A.; Shilov, A. E. Nitrogen fixation in solution. *Coord. Chem. Rev.* **1995**, *144*, 69–145.
- (34) *Activation of Small Molecules*, 1st ed.; Tolman, W. B., Ed.; Wiley-VCH: Weinheim, Germany, 2006.
- (35) MacKay, B. A.; Fryzuk, D. M. Dinitrogen coordination chemistry: on the biomimetic borderlands. *Chem. Rev.* **2004**, *104*, 385–401.
- (36) Vandersluys, W. G.; Burns, C. J.; Huffman, J. C.; Sattelberger, A. P. Uranium alkoxide chemistry. 1. Synthesis and the novel dimeric structure of the first homoleptic uranium(III) aryloxide complex. *J. Am. Chem. Soc.* **1988**, *110*, 5924–5925.
- (37) Arnold, P. L. Uranium-mediated activation of small molecules. *Chem. Commun.* **2011**, *47*, 9005–9010.
- (38) Macdonald, M. R.; Fieser, M. E.; Bates, J. E.; Ziller, J. W.; Furche, F.; Evans, W. J. Identification of the + 2 oxidation state for uranium in a crystalline molecular complex, [K(2.2.2-cryptand)]-[(C₅H₄SiMe₃)₃U]. *J. Am. Chem. Soc.* **2013**, *135*, 13310–13313.
- (39) La Pierre, H. S.; Kameo, H.; Halter, D. P.; Heinemann, F. W.; Meyer, K. Coordination and redox isomerization in the reduction of a uranium(III) monoarene complex. *Angew. Chem., Int. Ed.* **2014**, *53*, 7154–7157.
- (40) La Pierre, H. S.; Scheurer, A.; Heinemann, F. W.; Hieringer, W.; Meyer, K. Synthesis and characterization of a uranium(II) monoarene complex supported by δ backbonding. *Angew. Chem., Int. Ed.* **2014**, *53*, 7158–7162.
- (41) Billow, B. S.; Livesay, B. N.; Mokhtarzadeh, C. C.; McCracken, J.; Shores, M. P.; Boncella, J. M.; Odom, A. L. Synthesis and characterization of a neutral U(II) arene sandwich complex. *J. Am. Chem. Soc.* **2018**, *140*, 17369–17373.
- (42) Parry, J. S.; Cloke, F. G. N.; Coles, S. J.; Hursthouse, M. B. Synthesis and characterization of the first sandwich complex of trivalent thorium: a structural comparison with the uranium analogue. *J. Am. Chem. Soc.* **1999**, *121*, 6867–6871.
- (43) Langeslay, R. R.; Chen, G. P.; Windorff, C. J.; Chan, A. K.; Ziller, J. W.; Furche, F.; Evans, W. J. Synthesis, structure, and reactivity of the sterically crowded Th³⁺ complex (C₅Me₂)₃Th including formation of the thorium carbonyl, [(C₅Me₂)₃Th(CO)]-[BPh₄]. *J. Am. Chem. Soc.* **2017**, *139*, 3387–3398.
- (44) Huh, D. N.; Roy, S.; Ziller, J. W.; Furche, F.; Evans, W. J. Isolation of a square-planar Th(III) complex: synthesis and structure of [Th(OC₆H₂^tBu₂-2,6-Me-4)₄]¹⁻. *J. Am. Chem. Soc.* **2019**, *141*, 12458–12463.
- (45) Boronski, J. T.; Seed, J. A.; Hunger, D.; Woodward, A. W.; van Slageren, J.; Woole, A. J.; Natrajan, L. S.; Kaltsoyannis, N.; Liddle, S. T. A crystalline tri-thorium cluster with σ-aromatic metal–metal bonding. *Nature* **2021**, *598*, 72–75.
- (46) Nguyen, J. Q.; Anderson-Sanchez, L. M.; Moore, W. N. G.; Ziller, J. W.; Furche, F.; Evans, W. J. Replacing trimethylsilyl with triisopropylsilyl provides crystalline (C₃H₄SiR₃)₃Th complexes of Th(III) and Th(II). *Organometallics* **2023**, *42*, 2927–2937.
- (47) Guo, F.-S.; Tsoureas, N.; Huang, G.-Z.; Tong, M.-L.; Mansikkamäki, A.; Layfield, R. A. Isolation of a perfectly linear uranium(II) metallocene. *Angew. Chem., Int. Ed.* **2020**, *59*, 2299–2303.
- (48) Straub, M. D.; Ouellette, E. T.; Boreen, M. A.; Britt, R. D.; Chakarawet, K.; Douair, I.; Gould, C. A.; Maron, L.; Del Rosal, I.; Villarreal, D.; Minasian, S. G.; Arnold, J. A. A uranium(II) arene complex that acts as a uranium(I) synthon. *J. Am. Chem. Soc.* **2021**, *143*, 19748–19760.
- (49) Keener, M.; Shivaraam, R. A. K.; Rajeshkumar, T.; Tricoire, M.; Scopelliti, R.; Živković, I.; Chauvin, A. S.; Maron, L.; Mazzanti, M. Multielectron redox chemistry of uranium by accessing the +II oxidation state and enabling reduction to a U(I) synthon. *J. Am. Chem. Soc.* **2023**, *145*, 16271–16283.
- (50) Keerthi Shivaraam, R. A.; Keener, M.; Modder, D.; Rajeshkumar, T.; Živković, I.; Scopelliti, R.; Maron, L.; Mazzanti,

- M. A route to stabilize uranium(II) and uranium(I) synthons in multimetallic complexes. *Angew. Chem., Int. Ed.* **2023**, *62*, No. e202304051.
- (51) Fang, W.; Li, Y.; Zhang, T.; Rajeshkumar, T.; del Rosal, I.; Zhao, Y.; Wang, T.; Wang, S.; Maron, L.; Zhu, C. Oxidative addition of E–H (E = C, N) bonds to transient uranium(II) centers. *Angew. Chem., Int. Ed.* **2024**, *63*, No. e202407339.
- (52) Evans, W. J.; Kozimor, S. A.; Ziller, J. W. A Monometallic f element complex of dinitrogen: (C₃Me₃)₃U(η¹-N₂). *J. Am. Chem. Soc.* **2003**, *125*, 14264–14265.
- (53) Wilkinson, P. G.; Houk, N. B. Emission spectra of nitrogen in the vacuum ultraviolet. *J. Chem. Phys.* **1956**, *24*, 528–534.
- (54) Lu, E.; Atkinson, B. E.; Wooles, A. J.; Boronski, J. T.; Doyle, L. R.; Tuna, F.; Cryer, J. D.; Cobb, P. J.; Vitorica-Yrezabal, I. J.; Whitehead, G. F. S.; Kaltsoyannis, N.; Liddle, S. T. Back-bonding between an electron-poor, high-oxidation-state metal and poor π-acceptor ligand in a uranium(V)–dinitrogen complex. *Nat. Chem.* **2019**, *11*, 806–811.
- (55) Jori, N.; Moreno, J. J.; Shivaraam, R. A. K.; Rajeshkumar, T.; Scopelliti, R.; Maron, L.; Campos, J.; Mazzanti, M. Iron promoted end-on dinitrogen-bridging in heterobimetallic complexes of uranium and lanthanides. *Chem. Sci.* **2024**, *15*, 6842–6852.
- (56) Roussel, P.; Scott, P. Complex of dinitrogen with trivalent uranium. *J. Am. Chem. Soc.* **1998**, *120*, 1070–1071.
- (57) Fox, A. R.; Bart, S. C.; Meyer, K.; Cummins, C. C. Towards uranium catalysts. *Nature* **2008**, *455*, 341–349.
- (58) Fryzuk, M. D.; Love, J. B.; Rettig, S. J.; Young, V. G. Transformation of coordinated dinitrogen by reaction with dihydrogen and primary silanes. *Science* **1997**, *275*, 1445–1447.
- (59) Roussel, P.; Errington, W.; Kaltsoyannis, N.; Scott, P. Back bonding without σ-bonding: a unique π-complex of dinitrogen with uranium. *J. Organomet. Chem.* **2001**, *635*, 69–74.
- (60) Kaltsoyannis, N.; Scott, P. Evidence for actinide metal to ligand π backbonding. Density functional investigations of the electronic structure of [(NH₂)₃(NH₃)U]₂(μ₂-η²:η²-N₂). *Chem. Commun.* **1998**, 1665–1666.
- (61) Gardner, B. M.; Liddle, S. T. Uranium triamidoamine chemistry. *Chem. Commun.* **2015**, *51*, 10589–10607.
- (62) Huang, Q.-R.; Kingham, J. R.; Kaltsoyannis, N. The strength of actinide–element bonds from the quantum theory of atoms-in-molecules. *Dalton Trans.* **2015**, *44*, 2554–2566.
- (63) Odom, A. L.; Arnold, P. L.; Cummins, C. C. Heterodinuclear uranium/molybdenum dinitrogen complexes. *J. Am. Chem. Soc.* **1998**, *120*, 5836–5837.
- (64) Laplaza, C. E.; Johnson, M. J. A.; Peters, J. C.; Odom, A. L.; Kim, E.; Cummins, C. C.; George, G. N.; Pickering, I. J. Dinitrogen cleavage by three-coordinate molybdenum(III) complexes: mechanistic and structural data. *J. Am. Chem. Soc.* **1996**, *118*, 8623–8638.
- (65) Guo, F.-S.; Chen, Y.-C.; Tong, M.-L.; Mansikkamäki, A.; Layfield, R. A. Uranocenium: synthesis, structure, and chemical bonding. *Angew. Chem., Int. Ed.* **2019**, *58*, 10163–10167.
- (66) Barluzzi, L.; Giblin, S. R.; Mansikkamäki, A.; Layfield, R. A. Identification of oxidation state + 1 in a molecular uranium complex. *J. Am. Chem. Soc.* **2022**, *144*, 18229–18233.
- (67) Huh, D. N.; Ziller, J. W.; Evans, W. J. Chelate-free synthesis of the U(II) complex, [(C₃H₃(SiMe₃)₂)₃U]¹⁻, using Li and Cs reductants and comparative studies of La(II) and Ce(II) analogs. *Inorg. Chem.* **2018**, *57*, 11809–11814.
- (68) Cloke, F. N.; Hitchcock, P. B. Reversible binding and reduction of dinitrogen by a uranium(III) pentalene complex. *J. Am. Chem. Soc.* **2002**, *124*, 9352–9353.
- (69) Mansell, S. M.; Kaltsoyannis, N.; Arnold, P. L. Small molecule activation by uranium tris(aryloxides): experimental and computational studies of binding of N₂, coupling of CO, and deoxygenation insertion of CO₂ under ambient conditions. *J. Am. Chem. Soc.* **2011**, *133*, 9036–9051.
- (70) Mansell, S. M.; Farnaby, J. H.; Germeroth, A. I.; Arnold, P. L. Thermally stable uranium dinitrogen complex with siloxide supporting ligands. *Organometallics* **2013**, *32*, 4214–4222.
- (71) Batov, M. S.; del Rosal, I.; Scopelliti, R.; Fadaei-Tirani, F.; Zivkovic, I.; Maron, L.; Mazzanti, M. Multimetallic uranium nitride cubane clusters from dinitrogen cleavage. *J. Am. Chem. Soc.* **2023**, *145*, 26435–26443.
- (72) Camp, C.; Pécaut, J.; Mazzanti, M. Tuning uranium–nitrogen multiple bond formation with ancillary siloxide ligands. *J. Am. Chem. Soc.* **2013**, *135*, 12101–12111.
- (73) Falcone, M.; Chatelain, L.; Scopelliti, R.; Živković, I.; Mazzanti, M. Nitrogen reduction and functionalization by a multimetallic uranium nitride complex. *Nature* **2017**, *547*, 332–335.
- (74) Falcone, M.; Barluzzi, L.; Andrez, J.; Fadaei Tirani, F.; Zivkovic, I.; Fabrizio, A.; Corminboeuf, C.; Severin, K.; Mazzanti, M. The role of bridging ligands in dinitrogen reduction and functionalization by uranium multimetallic complexes. *Nat. Chem.* **2019**, *11*, 154–160.
- (75) Jori, N.; Rajeshkumar, T.; Scopelliti, R.; Živković, I.; Sienkiewicz, A.; Maron, L.; Mazzanti, M. Cation assisted binding and cleavage of dinitrogen by uranium complexes. *Chem. Sci.* **2022**, *13*, 9232–9242.
- (76) Jori, N.; Keener, M.; Rajeshkumar, T.; Scopelliti, R.; Maron, L.; Mazzanti, M. Dinitrogen cleavage by a dinuclear uranium(III) complex. *Chem. Sci.* **2023**, *14*, 13485–13494.
- (77) Arnold, P. L.; Ochiai, T.; Lam, F. Y. T.; Kelly, R. P.; Seymour, M. L.; Maron, L. Metallacyclic actinide catalysts for dinitrogen conversion to ammonia and secondary amines. *Nat. Chem.* **2020**, *12*, 654–659.
- (78) Wong, A.; Lam, F. Y. T.; Hernandez, M.; Lara, J.; Trinh, T. M.; Kelly, R. P.; Ochiai, T.; Rao, G.; Britt, R. D.; Kaltsoyannis, N.; Arnold, P. L. Catalytic reduction of dinitrogen to silylamines by earth-abundant lanthanide and group 4 complexes. *Chem. Catalysis* **2024**, *4*, No. 100964.
- (79) Green, D. W.; Reedy, G. T. The identification of UN in Ar matrices. *J. Chem. Phys.* **1976**, *65*, 2921–2922.
- (80) Hunt, R. D.; Yustein, J. T.; Andrews, L. Matrix infrared spectra of NUN formed by the insertion of uranium atoms into molecular nitrogen. *J. Chem. Phys.* **1993**, *98*, 6070–6074.
- (81) Kushto, G. P.; Souter, P. F.; Andrews, L. An infrared spectroscopic and quasirelativistic theoretical study of the coordination and activation of dinitrogen by thorium and uranium atoms. *J. Chem. Phys.* **1998**, *108*, 7121–7130.
- (82) Andrews, L.; Wang, X.; Lindh, R.; Roos, B. O.; Marsden, C. J. Simple N≡UF₃ and P≡UF₃ molecules with triple bonds to uranium. *Angew. Chem., Int. Ed.* **2008**, *47*, 5366–5370.
- (83) Andrews, L.; Wang, X.; Gong, Y.; Kushto, G. P.; Vlaisavljevich, B.; Gagliardi, L. Infrared spectra and electronic structure calculations for NN complexes with U, UN, and NUN in solid argon, neon, and nitrogen. *J. Phys. Chem. A* **2014**, *118*, 5289–5303.
- (84) Li, F.; Qin, J.; Qiu, R.; Shuai, M.; Pu, Z. Matrix-isolation infrared spectra and electronic structure calculations for dinitrogen complexes with uranium trioxide molecules UO₃(η¹-NN)_{1–4}. *Inorg. Chem.* **2022**, *61*, 11075–11083.
- (85) Korobkov, I.; Gambarotta, S.; Yap, G. P. A. A highly reactive uranium complex supported by the calix[4]tetrapyrrole tetraanion affording dinitrogen cleavage, solvent deoxygenation, and polysilanol depolymerization. *Angew. Chem., Int. Ed. Engl.* **2002**, *41*, 3433–3436.
- (86) Korobkov, I.; Gambarotta, S.; Yap, G. P. A. Amide from dinitrogen by in situ cleavage and partial hydrogenation promoted by a transient zero-valent thorium synthon. *Angew. Chem., Int. Ed.* **2003**, *42*, 4958–4961.
- (87) Wang, P.; Douair, I.; Zhao, Y.; Wang, S.; Zhu, J.; Maron, L.; Zhu, C. Facile dinitrogen and dioxygen cleavage by a uranium(III) complex: cooperativity between the non-Innocent ligand and the uranium center. *Angew. Chem., Int. Ed.* **2021**, *60*, 473–479.
- (88) Morello, L.; Yu, P.; Carmichael, C. D.; Patrick, B. O.; Fryzuk, M. D. Formation of phosphorus–nitrogen bonds by reduction of a titanium phosphine complex under molecular nitrogen. *J. Am. Chem. Soc.* **2005**, *127*, 12796–12797.
- (89) Mo, Z.; Shima, T.; Hou, Z. Synthesis and diverse transformations of a dinitrogen dititanium hydride complex bearing rigid

acidane-based PNP-pincer ligands. *Angew. Chem., Int. Ed.* **2020**, *59*, 8635–8644.

(90) Feng, G.; Zhang, M.; Shao, D.; Wang, X.; Wang, S.; Maron, L.; Zhu, C. Transition metal bridged bimetallic clusters with multiple uranium-metal bonds. *Nat. Chem.* **2019**, *11*, 248–253.

(91) Feng, G.; Zhang, M.; Wang, P.; Wang, S.; Maron, L.; Zhu, C. Identification of a uranium–rhodium triple bond in a heterometallic cluster. *Proc. Natl. Acad. Sci. U. S. A.* **2019**, *116*, 17654–17658.

(92) Sheng, W.; Rajeshkumar, T.; Zhao, Y.; Maron, L.; Zhu, C. Electronic delocalization and σ -aromaticity in heterometallic cluster with multiple thorium-palladium bonds. *J. Am. Chem. Soc.* **2024**, *146*, 12790–12798.

(93) Feng, G.; McCabe, K. N.; Wang, S.; Maron, L.; Zhu, C. Construction of heterometallic clusters with multiple uranium-metal bonds by dianionic nitrogen-phosphorus ligands. *Chem. Sci.* **2020**, *11*, 7585–7592.

(94) Shen, J.; Rajeshkumar, T.; Feng, G.; Zhao, Y.; Wang, S.; Maron, L.; Zhu, C. Complexes featuring a *cis*-[MUM] core (M = Rh, Ir): A new route to uranium-metal multiple bonds. *Angew. Chem., Int. Ed.* **2023**, *62*, No. e202303379.

(95) Fang, W.; Zhu, Q.; Zhu, C. Recent advances in heterometallic clusters with f-block metal-metal bonds: synthesis, reactivity and applications. *Chem. Soc. Rev.* **2022**, *51*, 8434–8449.

(96) Zhu, Q.; Fang, W.; Maron, L.; Zhu, C. Heterometallic clusters with uranium–metal bonds supported by double-layer nitrogen–phosphorus ligands. *Acc. Chem. Res.* **2022**, *55*, 1718–1730.

(97) Xin, X.; Douair, I.; Zhao, Y.; Wang, S.; Maron, L.; Zhu, C. Dinitrogen cleavage by a heterometallic cluster featuring multiple uranium-rhodium bonds. *J. Am. Chem. Soc.* **2020**, *142*, 15004–15011.

(98) Xin, X.; Douair, I.; Zhao, Y.; Wang, S.; Maron, L.; Zhu, C. Dinitrogen cleavage and hydrogenation to ammonia with a uranium complex. *Natl. Sci. Rev.* **2023**, *10*, No. nwac144.

(99) Jori, N.; Barluzzi, L.; Douair, I.; Maron, L.; Fadaei-Tirani, F.; Živković, I.; Mazzanti, M. Stepwise reduction of dinitrogen by a uranium–potassium complex yielding a U(VI)/U(IV) tetranitride cluster. *J. Am. Chem. Soc.* **2021**, *143*, 11225–11234.

(100) Keener, M.; Fadaei-Tirani, F.; Scopelliti, R.; Živković, I.; Mazzanti, M. Nitrogen activation and cleavage by a multimetallic uranium complex. *Chem. Sci.* **2022**, *13*, 8025–8035.